EuroIntervention
2025;21:e778-e795
published online e-edition July 2025
DOI: 10.4244/EIJ-D-24-00387

State-of-the-Art
by EuroIntervention

Advances in coronary imaging of atherosclerotic plaques

Héctor M. García-García[1]*, MD, PhD; Jorge Sanz-Sánchez[2,3], MD, PhD; Natalia Pinilla-Echeverri[4,5], MD, PhD; Pablo J. Blanco[6], BSc, PhD; Christos Bourantas[7,8], MD, PhD; Fernando Alfonso[9], MD, PhD

**Corresponding author: Section of Interventional Cardiology, MedStar Washington Hospital Center, 110 Irving Street NW, Suite 4B-1, Washington, D.C., 20010, USA. E-mail: hector.m.garciagarcia@medstar.net*

This paper also includes supplementary data published online at: https://eurointervention.pcronline.com/doi/10.4244/EIJ-D-24-00387

ABSTRACT

Atherosclerosis is a complex disease with multiple factors associated with its progression and complications. Fibroatheroma is a pathological entity which contains abundant lipid, and often, a thin fibrous cap that is the most common underlying cause of acute myocardial infarction. Based on pathological descriptions, we propose a new imaging-based nomenclature indicating high-risk plaque characteristics that can be identified with imaging. Additionally, we review the literature indicating *in vivo* plaque characterisation as well as outlining the natural history of plaques and, more importantly, its responses to systemic and local therapies. Intravascular imaging has positively impacted how we evaluate atherosclerosis, and it can provide guidance on the use of tailored therapies and the evaluation of their long-term follow-up effects.

Imaging of the coronary atherosclerotic process has provided unique insights into the natural history of coronary artery disease (CAD) and has allowed us to better understand the mechanisms regulating plaque evolution. Efforts have been made over recent years to identify plaque prone to thrombosis and to detect plaque characteristics that are associated with a high risk of vascular complications and clinical events. Furthermore, the imaging of plaque pathology has allowed us to evaluate the systemic and local effects of existing and emerging treatments developed to inhibit plaque progression.

This review aims to facilitate a comprehensive assessment of plaque pathology using coronary imaging. We first describe the use of imaging to characterise the individual plaque components and how they coexist and form different plaque phenotypes; we then present the plaque features associated with clinical events. Finally, we summarise the pharmacological clinical trials that used serial imaging methods to evaluate the effect of established and newly developed drugs on plaque morphology and progression/regression **(Central illustration)**.

How to assess atherosclerotic plaque size and its components

The most used coronary imaging modalities are either non-invasive, such as coronary computed tomography angiography (CCTA), or invasive, such as intravascular ultrasound (IVUS) or optical coherence tomography (OCT) and their combination with near-infrared spectroscopy (NIRS).

PLAQUE

Plaque (also known as atheroma) refers to the material located between the lumen area (at the interface between the space where the blood flows and the vessel wall) and the outermost (trailing) edge of the media, which coincides with the location of the external elastic membrane (EEM) or lamina (EEL).

Plaque burden is the preferred metric to describe the relative amount of plaque area that is contained within the vessel area and is defined as the plaque area divided by the vessel area (reported as a percentage).

Plaque components determine its vulnerability; the following tissue types can be detected by coronary imaging **(Supplementary Table 1)**.

LIPID CORE AND NECROTIC CORE

Lipid plaque and necrotic core tissue **(Figure 1, Moving image 1)** were described by Rudolf Virchow, who used the term "atheroma" to describe a dermal cyst consisting of a fatty mass encapsulated within the fibrous cap, analogous to the capsule containing an abscess, that is vulnerable to rupture[1]. NIRS is the only imaging modality that is validated

KEYWORDS: atherosclerosis; coronary computed tomography angiography; intravascular ultrasound; optical coherence tomography

SUBMITTED ON 25/04/2024 - REVISION RECEIVED ON 1st 16/09/2024 / 2nd 07/01/2025 / 3rd 27/02/2025 - ACCEPTED ON 31/03/2025

EuroIntervention Central Illustration

Imaging assessment of atherosclerotic plaque.

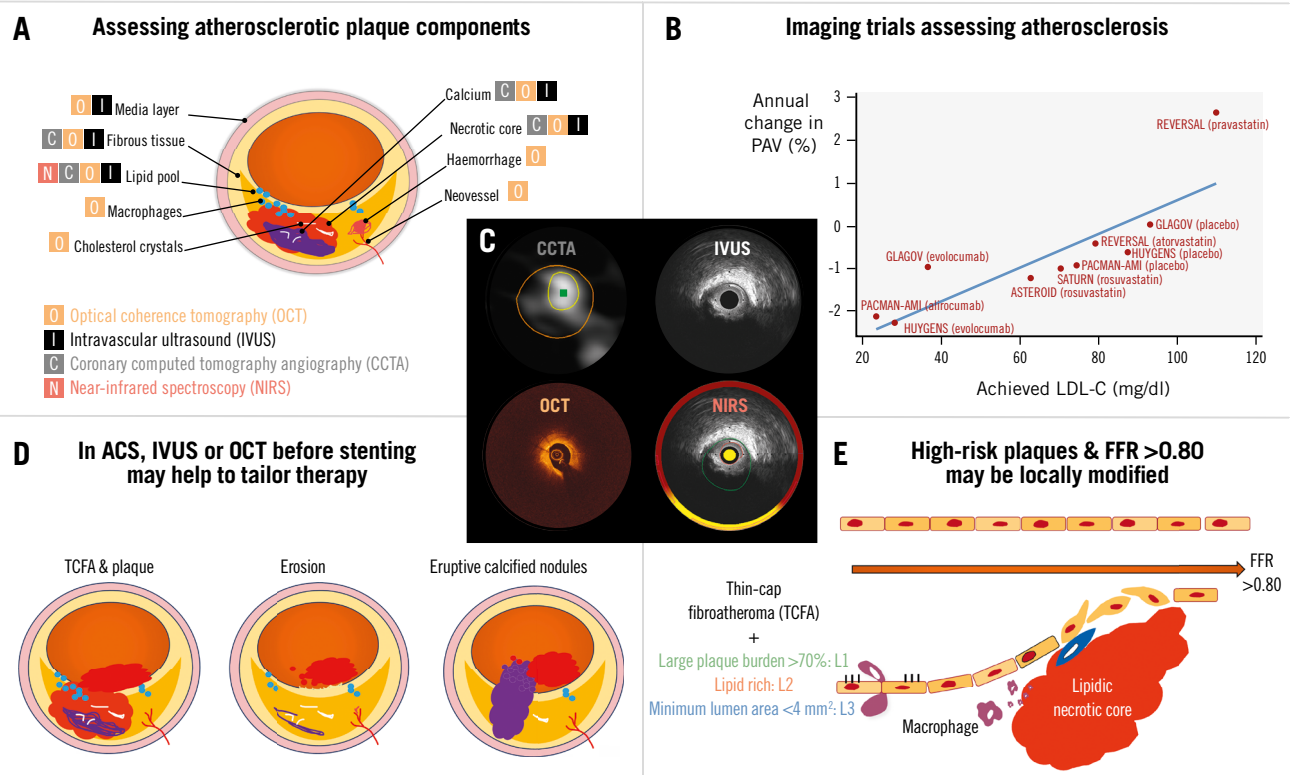

Héctor M. García-García *et al.* • *EuroIntervention* 2025;21:e778-e795 • DOI: 10.4244/EIJ-D-24-00387

A) Assessment of coronary plaque size and its components is possible using non-invasive or invasive imaging methods. B) Traditionally, serial IVUS studies have been used to assess the impact of systemic medications on plaque changes. The graph shows a selected number of studies with respect to the average change in PAV against the achieved LDL-C. C) Four images of a lipid-rich plaque with a large plaque burden and a small lumen area in a single coronary location of one patient imaged by coronary computed tomography angiography (CCTA; non-invasive), intravascular ultrasound (IVUS; invasive), optical coherence tomography (OCT; invasive) and near-infrared spectroscopy (NIRS; invasive). D) Intracoronary imaging has helped us to understand the pathophysiology of acute coronary syndromes (ACS) with respect to the underlying cause of the coronary thrombosis. For rupture and thin-cap fibroatheroma (TCFA), drug-eluting stents (DES) are the most common local treatment; drug-coated balloons (DCBs) are emerging as an alternative, but confirmatory studies are still ongoing. E) Patients with uncomplicated plaques that portray high-risk characteristics (i.e., large plaque burden, lipid-rich and reduced lumen area), but fractional flow reserve (FFR) >0.80, are being randomised to test whether pre-emptive local therapies, either stents or DCBs, can modify their natural history. LDL-C: low-density lipoprotein cholesterol; PAV: percentage atheroma volume

and approved for detection of lipid in the vasculature. NIRS is included in hybrid imaging probes: IVUS/NIRS or OCT/NIRS.

NIRS presents the data in a chemogram, a two-dimensional map of the plaque composition. Segments with a high probability of having lipid cores are shown in yellow, while those with a low probability of lipid are displayed in red. NIRS data are summarised as the lipid core burden index (LCBI), which is the amount of lipid in a scanned artery, and the maximum LCBI within any 4 mm pullback length ($LCBI_{4mm}$) is commonly used to represent the amount of lipid in a coronary segment of 4 mm length[2] **(Figure 1, Moving image 1)**.

Greyscale IVUS or OCT, used without NIRS, as well as CCTA can also detect lipid contents **(Figure 1, Moving image 1)**.

More specifically, on IVUS, hypoechogenic (also named echolucent) and attenuated plaques have been associated with lipid and necrotic core content in histological studies[3-5]. However, greyscale IVUS is less accurate than NIRS in identifying lipid tissue and, in addition to that, there is high interobserver variability in the reading/interpretation of

IVUS for plaque phenotypes[6]. Therefore IVUS/NIRS should be preferred over greyscale IVUS alone for the detection of lipid-laden plaques[3].

Virtual histology IVUS (VH-IVUS) use is limited to a few clinical centres worldwide. It visualises 4 distinct plaque components: fibrous (depicted in dark green), fibrofatty (light green), necrotic core (red), and calcium (white)[7]. Using VH-IVUS, fibroatheroma is defined by the presence of >10% confluent necrotic core. Thin-cap fibroatheroma (TCFA) is said to be present if more than 36 degrees (30 degrees in the PREVENT study – see below[8]) of the necrotic core is in direct contact with the lumen in 3 or more consecutive frames; otherwise it is defined as thick-cap fibroatheroma. VH-IVUS is limited, however, in terms of assessing fibrous cap thickness (FCT) because of its poor axial resolution **(Figure 1B, Moving image 1)**.

OCT lipidic pool and necrotic core are defined as a hyporeflective (low-signal) region with diffuse borders that is covered by a fibrous cap which has a high signal attenuation[9]. The thickness of the fibrous cap is used to classify lipid-rich plaques as thin- (TCFA – cutoff of <65 µm) or thick-cap fibroatheromas. For reproducible fibrous cap thickness analysis, we propose the use of automated software developed for this purpose instead of a manual measurement.

CCTA uses attenuation, expressed in Hounsfield units (HU), to differentiate between calcified plaques with higher attenuation and non-calcified plaques with lower attenuation. The recommended threshold for the definition of low-attenuation plaques is <30 HU, although attenuation is affected by some CCTA acquisition parameters such as lumen attenuation and tube voltage. These plaques have been shown to correlate with lipid-rich plaques assessed by IVUS in relatively small studies[10-12] **(Figure 1A, Moving image 1)**.

CALCIUM

Coronary angiography has low to moderate sensitivity compared to IVUS, OCT, or CCTA to identify coronary calcification[13].

On IVUS, calcium is shown as a hyperechoic (echodense) structure brighter than the reference adventitia with shadowing of deeper vascular tissue structures. IVUS has high sensitivity (89-90%) and specificity (97-100%) for detecting calcium deposits within a plaque[13]. However, it has shown limited sensitivity (64%) in visualising accumulation of microcalcification (≤0.05 mm)[14] (**Figure 2, Moving image 2**).

Qualitative assessment includes the evaluation of the distribution patterns of coronary calcification:
(a) superficial: the leading edge of acoustic shadowing is within the shallowest 50% of the plaque and media thickness.
(b) deep: the leading edge of acoustic shadowing is within the deepest 50% of the plaque and media thickness[13].

As an ultrasound beam cannot penetrate calcium, the thickness of its reflection in a greyscale IVUS image is a function of transducer saturation by the reflected ultrasound energy and not by the real anatomical thickness[13]. Therefore, calcium thickness, area, and volume cannot be measured by IVUS. Nevertheless, the presence of a smooth surface with reverberations (secondary false concentric echoes at reproducible distances between the IVUS transducer and the calcium leading edge) has been associated with thin calcium by OCT[15].

In OCT evaluation, calcium is hyporeflective (i.e., a signal-poor, dark region) with sharply delineated borders. OCT has shown a sensitivity for the detection of calcium ranging between 85.4% and 96% and a specificity of 97-100% using pathology as a gold standard[14]. In a head-to-head comparison between IVUS and OCT, Wang et al reported that in 13.2% of IVUS-detected calcium, calcium was either not visible by OCT or was underestimated due to superficial OCT plaque attenuation[14] **(Figure 2, Moving image 2)**.

In contrast to IVUS, OCT can penetrate calcium and in most cases visualise its trailing edge, thereby allowing a three-dimensional assessment by evaluating (a) angle (degrees), (b) length (measured in mm), and (c) thickness (measured in mm), and, therefore, its area and volume[16].

Calcium burden, assessed by IVUS or OCT, is important for percutaneous coronary intervention (PCI) planning, and algorithms (some using artificial intelligence [AI]) have been developed and validated that predict stent underexpansion with accuracy[18-20] **(Figure 2, Moving image 2)**.

Coronary artery calcium (CAC) assessment by CCTA, reported as a calcium score, has been shown to be a strong predictor for incident cardiovascular disease events and is currently considered a reliable surrogate marker for screening of CAD[21]. The Agatston scoring method is one of the most common methods used for CAC scoring, and a calcium score of 0 has been reported to reflect a very low risk for cardiovascular events, especially in asymptomatic patients. However, due to the limited spatial resolution of computed tomography (CT) scans, a zero CAC score does not eliminate the possibility of calcium flecks or softer plaques[21,22].

In addition to cardiovascular risk assessment, CCTA provides an accurate characterisation of coronary atherosclerosis (i.e., plaque burden, plaque volume, tissue characterisation)[22,23]. However, severe calcification can limit lumen assessment due to blooming artefacts and yield an overestimation of lesion severity, thus decreasing the specificity of CCTA, although photon-counting CT has fewer artefacts. Calcium can be reported based on CCTA as (a) angle (degrees) and (b) length (mm). Thickness and area are also impacted by blooming artefacts.

Finally, CCTA has the potential to identify microcalcifications, which have been suggested to be a frequent feature in some unstable plaques. In CCTA, spotty calcification is defined as a small, dense (>130 HU) plaque component surrounded by non-calcified plaque tissue. The cutoff to define a calcification in CCTA as spotty is <3 mm[22,23]. Small spotty calcification has the strongest association with vulnerable plaque features defined by IVUS[24].

FIBROUS TISSUE

In early phases of the disease, fibrous tissue is the most prevalent tissue type in atherosclerotic plaques[7]. By IVUS, it is recognised as a homogeneous and normoechogenic structure, while on OCT it shows as a bright, hyperreflective tissue.

MACROPHAGES

By OCT, macrophages appear as confluent multiple bright spots which cast dorsal shadowing[9]. Histopathology studies

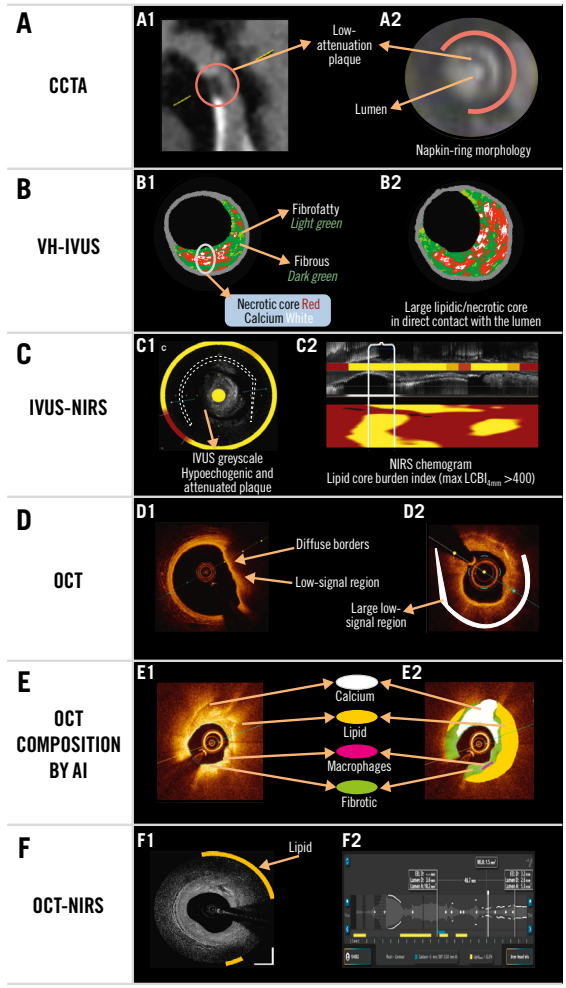

Figure 1. *Lipid- and necrotic core-rich plaques. Examples of lipid-rich plaques using different imaging modalities. A) Coronary computed tomography angiography (CCTA). A1) Plaque with low Hounsfield units (HU) which corresponds to a napkin-ring morphology plaque, as shown in the cross-section (A2). B) Virtual histology (VH)-intravascular ultrasound (IVUS) shows 4 tissue types; the large amount of necrotic core abutting the lumen is suggestive of thin-cap fibroatheroma. C) IVUS near-infrared spectroscopy (NIRS) shows cholesterol content regions in yellow on the same IVUS frame (C1) and on the chemogram (C2; shown below the longitudinal IVUS view) representing the entire length of the imaged vessel; a lipid core burden index (LCBI) >400 is deemed to confer high risk for future events. D) Optical coherence tomography (OCT) indirectly provides insights into lipid content in the vessel wall. Hyporeflective (low-signal) sectors with diffuse borders have been associated with lipid content. E) Artificial intelligence (AI) algorithms applied to OCT images colour code the tissue contents of the vessel wall. F) OCT in combination with NIRS is also available. F1) An OCT frame: the yellow arc indicates the sector in which the lipid is located. F2) The longitudinal viewport: the lipid colour bar shows the longitudinal location where lipid is ≥user-defined threshold (**Moving image 1, Supplementary Figure 1, Supplementary Table 1**).*

showed that OCT can detect the presence of macrophages over a fibrous cap, but it has a limited efficacy in identifying these microstructrures across the entire plaque. AI methods have been introduced to improve the reproducibility of macrophage detection[25], as a recent report has also shown moderate to low correlation between the estimations of experts using two different OCT catheters[26]. Thus, it is highly recommended to take into account the limited precision of the modality when reporting the presence of macrophages in OCT images.

CHOLESTEROL CRYSTALS

Cholesterol crystals appear as bright (with high reflectivity), sharp and well-delineated lines, without a clear dorsal shadow; they are sometimes multiple and stacked on top of each other. In comparison with histology, OCT has low to moderate sensitivity but high specificity for detecting these components[27].

MICROVESSELS

Microvessels are small (diameter of 50-300 μm) voids that are well demarcated, tend to concentrate in the intima, and have the same appearance as the lumen (signal-poor). They are present in multiple contiguous frames (>3) and can be seen to communicate with the lumen and/or with the adventitia. Three-dimensional OCT can show the complete network[28]. A histology study showed moderate sensitivity and specificity of the modality to detect plaque vascularisation (52% and 68%, respectively)[29].

THROMBUS

Thrombus is a mass prolapsing and/or floating into the lumen and is easily detected by OCT[30]; thrombus may be attached to the lumen and, in this setting, is usually mixed with some other tissue and may be hard to delineate. There are three types: red thrombus (erythrocyte-abundant), which is hyperreflective at the rim facing the OCT catheter and attenuated with dorsal shadowing in its depth; white thrombus (platelet-abundant), which is homogeneous with low attenuation; and mixed thrombus, which portrays a combination of both red and white thrombi characteristics[9] **(Figure 3, Moving image 3)**. Due to its unsurpassed resolution, OCT is currently considered the gold standard for the diagnosis of intracoronary thrombus.

IVUS can also recognise intraluminal masses which appear heterogeneous (i.e., present with different echogenicities) as well as those with different degrees of attenuation depending on their age and composition[31]. However, precise recognition may be challenging because of its limited resolution. It is, therefore, highly recommended to use moving images (i.e., loop or dynamic review, or simply go back and forth frame by frame) to better detect it and delineate thrombus extension; the latter may be difficult, however, if the thrombus is attached to the wall since thrombus may appear as a continuum with the underlying plaque.

CCTA has limited capabilities for thrombus detection. Thrombus appears as an irregular-shaped plaque with significant intraluminal protrusion[32,33]. Similarly to OCT and IVUS, CCTA cannot distinctively measure thrombus as it is mixed with the underlying plaque. Therefore, it is often

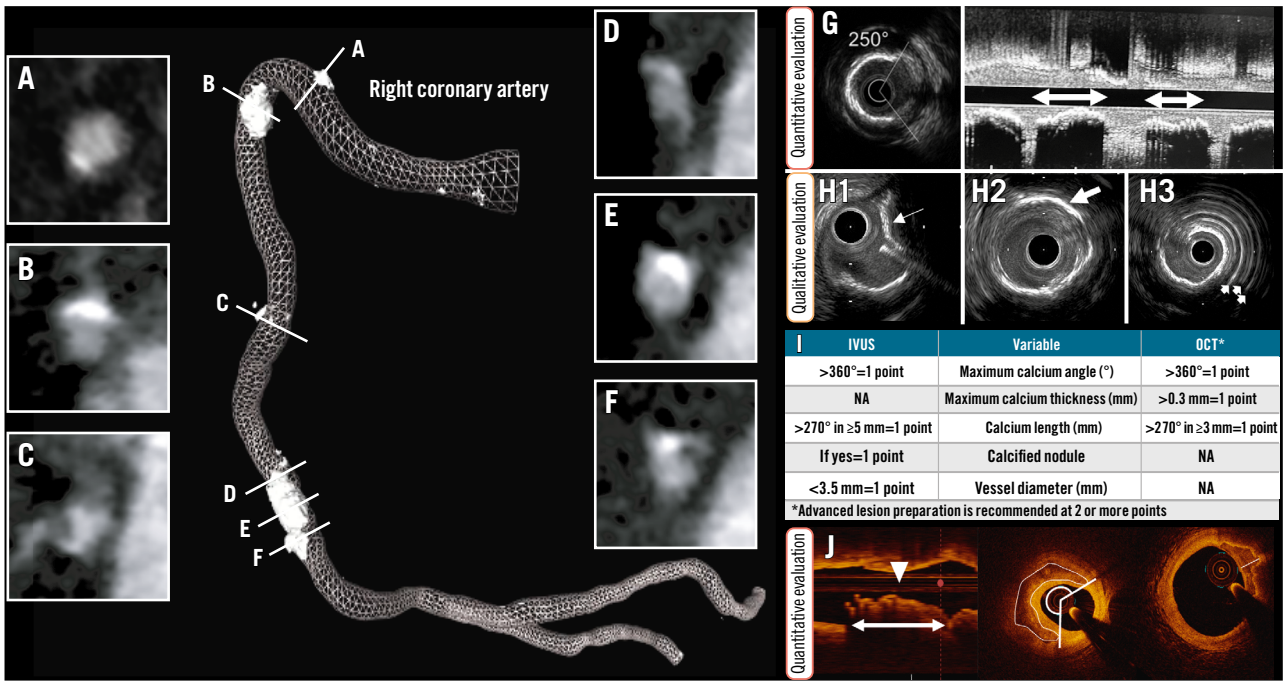

I	IVUS	Variable	OCT*
	>360°=1 point	Maximum calcium angle (°)	>360°=1 point
	NA	Maximum calcium thickness (mm)	>0.3 mm=1 point
	>270° in ≥5 mm=1 point	Calcium length (mm)	>270° in ≥3 mm=1 point
	If yes=1 point	Calcified nodule	NA
	<3.5 mm=1 point	Vessel diameter (mm)	NA

*Advanced lesion preparation is recommended at 2 or more points

Figure 2. *Calcified plaques. Non-invasive, coronary computed tomography angiography (left) provides information about the extent of calcification. The right coronary artery image shows the lumen profile (mesh) and the length of spots of calcification. Cross-sectional views from (A) to (F) depict the circumferential extent of calcium. From these images, the angle, density, area and thickness of the calcium can be measured. G) By intravascular ultrasound (IVUS), the arc and the length of calcium can be measured. H) Further, the nodular appearance (H1; white arrow) and location within the plaque such as deep calcium (H2; white arrow) and superficial calcium (H3; white arrows represent the reverberations from the superficial calcium) can be identified. J) By optical coherence tomography (OCT) also, the length, area, and thickness of calcification can be quantified. These variables have been used to derive two calcium scores, as shown in (I).* ***(Moving image 2)****. NA: not applicable*

measured all together as plaque burden and the HU can be used to indicate the heterogeneous composition **(Figure 3, Moving image 3)**.

Plaque phenotypes

Intravascular imaging studies have adopted, non-systematically, some pathological terms to describe the appearance of the plaques, e.g., TCFA, which mimics pathological descriptions. We therefore propose that all intravascular imaging-defined plaque types consistently follow the relevant pathological descriptions **(Figure 4, Moving image 4)**.

In addition, we propose that the plaque's name should emphasise the coexistence of some plaque characteristics which have been shown to be prognostically relevant. These are (i) a Large plaque burden (>70%), which is the strongest predictor of future events and therefore will be named "L1"; (ii) a Lipid-rich composition, which will be indicated by "L2"; this will be used when, by OCT/IVUS, the hyporeflective/hypoechogenic region with diffuse contours is >1 quadrant, or, by NIRS, the maximum LCBI is >400; and (iii) a small Lumen area, which will be indicated if the minimum lumen area of the lesion is <4 mm^2, named "L3" **(Figure 5, Moving image 5)**.

PATHOLOGICAL INTIMAL THICKENING

By IVUS, pathological intimal thickening (PIT) is mostly normo- or hyperechogenic, alluding to its predominant fibrotic composition. We propose adding "plus" or "+" with "L1" and/or "L3" to the name if a large plaque burden and reduced lumen are present.

By OCT, it is mostly hyperreflective. "Plus" or "+" with "L1" and/or "L3" may be added accordingly.

FIBROATHEROMA

All fibroatheromas (FAs) are lipid-rich plaques, and therefore "L2" may or may not be added to the name.

By IVUS, an FA is a mixed plaque consisting of some hyperechogenic tissue and more than one quadrant of hypoechogenic tissue; this sector containing the hypoechogenic tissue may have some attenuation.

We propose adding "plus" or "+" and "L1" to the name when plaque burden is more than 70% and/or "L3" when the minimum lumen area <4 mm^2.

By OCT, an FA is also a mixed plaque appearing as hyperreflective tissue and more than one quadrant of hyporeflective tissue; we also propose adding "plus" or "+" and "L1" to the name when plaque burden is more than

70% (for newer-generation OCT technologies) or "L3" if a minimum lumen area <4 mm^2 is present.

THIN-CAP FIBROATHEROMA

TCFA is defined as a lipid plaque covered by a thin (<65 µm) fibrous cap. Similarly, we propose adding "plus" or "+" and "L1" to the name when the plaque burden is >70% or "L3" when a minimum lumen area <4 mm^2 is present. For a plaque to be called a "fibroatheroma", a large lipid content is required.

FIBROCALCIFIC

The term fibrocalcific (FC) describes mixed plaque in which dense calcium is present in more than one quadrant. These plaques may also portray a large plaque burden (L1), lipid-rich sectors (L2), or a reduced minimum lumen area (L3), and these specific traits should be noted in the plaque name, for example, FC plus L1 and L3, etc.

PLAQUE RUPTURE

Plaque rupture (PR) presents as a plaque ulceration (cavity) with a tear detected in a fibrous cap. Its cavity within the plaque communicates with the lumen with or without an overlying fibrous cap fragment. OCT is the best technique to detect PR, but not all plaque ruptures are detected by greyscale IVUS or OCT because the cavity is often filled with thrombus **(Figure 3, Moving image 3)**.

PLAQUE EROSION

Currently plaque erosion (PE) cannot be reliably diagnosed by IVUS, NIRS, or CCTA due to their limited resolution. OCT has an unsurpassed resolution, but it is still insufficient for visualising the endothelial lining. Therefore, the pathological definition of erosion cannot simply be adapted for the OCT definition **(Figure 3E, Moving image 3)**.

We therefore suggest the following definition of plaque erosion: a thrombotic lesion without fibrous cap disruption when coronary embolism has been ruled out.

There have been other definitions of PE in the literature. 1) A culprit lesion with or without an intact fibrous cap, emphasising that visualisation of the endothelial layer was not possible in eroded plaques, despite its unique axial resolution[3]. 2) Another definition proposed using the term "OCT-erosion" instead of erosion. "OCT-erosion" was defined and categorised according to the absence of fibrous cap disruption associated with the presence of thrombus. "Definite" OCT-erosion was defined as the presence of attached thrombus overlying an intact and visible plaque. Alternatively, "probable" OCT-erosion was defined by (1) luminal surface irregularity at the culprit lesion in the absence of thrombus or (2) attenuation of underlying plaque by thrombus without superficial lipid or calcification immediately proximal or distal to the site of thrombus. This is in clear contrast to the pathological definition of erosion that requires the presence of attached thrombus[34]. In the clinical setting, however, we may assume in some cases that thrombus might have vanished by the time of the imaging.

We acknowledge that there is an inherent limitation of OCT for the diagnosis of plaque erosion, and that is the presence of significant thrombus overlying the culprit lesion, which may prevent visualisation (due to shadowing) of an underlying plaque rupture. However, the predominant type of thrombus in patients with plaque erosion (75% of patients) is white thrombus, which should not obscure the underlying plaque. However, these definitions remain highly controversial, and the risk of OCT overdiagnosis exists. Too many different types of plaques are probably lumped together in the intact fibrous cap category. Likewise, the advancement of thromboaspiration catheters may disrupt not only thrombus but also the underlying plaque. It remains impossible to ascertain whether some of the observed plaque ruptures are spontaneous or rather a result of a mechanical trauma (including a Dotter effect) on thin- or thick-cap fibroatheromas. Iatrogenic mechanical disruption of the culprit lesion by bulky thromboaspiration catheters remains a possible reason for misclassification.

ERUPTIVE CALCIFIED NODULES

By IVUS evaluation, eruptive calcified nodules (ECNs) appear as a convex calcified shape of the luminal surface with irregular leading edges **(Figure 2, Moving image 2)**. Thrombus overlying this plaque may not be visualised by IVUS due to its limited resolution.

By OCT, ECNs appear as confined superficial calcification protruding into the lumen with disruption of the fibrous cap and associated thrombosis.

Thus, in describing plaque, the term ECN is exclusively to be used for "complicated" ECNs which are associated with thrombus and disruption of the overlying cap[35]. Some ECNs may actually also induce major dorsal shadowing on OCT[9]. This is in line with the pathological description in which a definition of ECN requires the presence of fibrous cap disruption and luminal thrombus.

NON-ERUPTIVE CN (NODULAR CALCIFICATION)

Nodular calcification has a similar appearance to an ECN, but it has an intact fibrous cap (i.e. non-eruptive), and in some lesions with stable protruding nodular calcifications, a bright leading edge with dorsal shadow may mimic an overlying thrombus and generate a misdiagnosis of an eruptive CN. However, the surface of a true eruptive CN tends to be more irregular, which allows, together with the clinical scenario, the correct diagnosis in most situations.

INTRAPLAQUE HAEMORRHAGE

We propose the following definitions to standardise reporting, but note some considerations in the subsequent paragraph:

By OCT, intraplaque haemorrhage appears as a hyporeflective core without dorsal attenuation.

By IVUS, intraplaque haemorrhage presents as a hypoechogenic core without attenuation.

Plaque haemorrhage is frequently seen in pathological specimens but its recognition by intracoronary imaging remains challenging. A pathological study evaluated 101 coronary arteries from 56 autopsy hearts using 40 MHz IVUS and NIRS and compared the imaging findings to histopathology. Segments with intraplaque haemorrhage had more fibroatheromas with a greater IVUS plaque burden, a greater prevalence of IVUS echolucent zones, and a higher NIRS lipid core burden index[36].

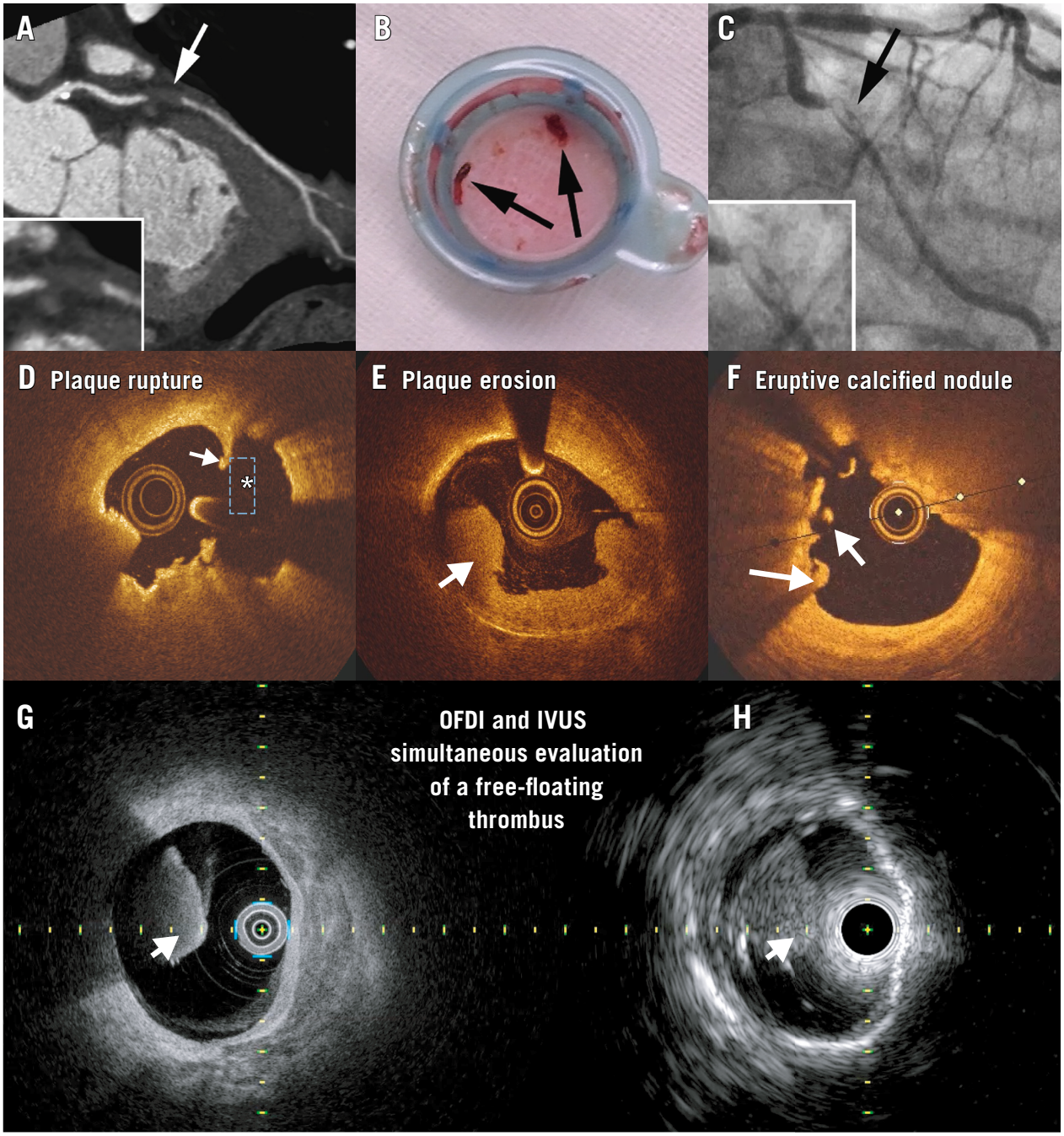

Figure 3. *Thrombotic lesions. A-C) A case example of a patient admitted for chest pain who was imaged with coronary computed tomography angiography (A), which showed the lumen was occupied with a low Hounsfield unit lesion. On the same day, the patient was diagnosed with coronary thrombosis, as shown in (B) and (C). D-H) Optical coherence tomography examples of red thrombus (white arrow) in a patient with a ruptured plaque (D). The asterisk shows the cavity, and the white arrow indicates the remnants of the fibrous cap. White thrombus is seen in (E), and (F) shows one floating mass and another mass attached to the vessel overlying an eruptive calcified nodule. The Dual Sensor hybrid IVUS-OCT catheter system was developed by Terumo (Japan) by merging IVUS and optical frequency domain imaging (OFDI) probes. G,H) A red thrombus simultaneously imaged with this Dual Sensor system. (**Moving image 3**). A-C) Adapted with permission from*[33]*. G,H) reproduced with permission from Terumo, Tokyo, Japan. IVUS: intravascular ultrasound; OCT: optical coherence tomography*

The combined use of high-definition IVUS and OCT appears to be able to provide better intraplaque resolution and some important diagnostic clues in patients with intraplaque haemorrhage. Nevertheless, new studies are required to understand what are the best morphological criteria required for the diagnosis of intraplaque haemorrhage and whether intracoronary imaging is still simply unable to obtain a reliable diagnosis of this challenging anatomical entity in our patients[37].

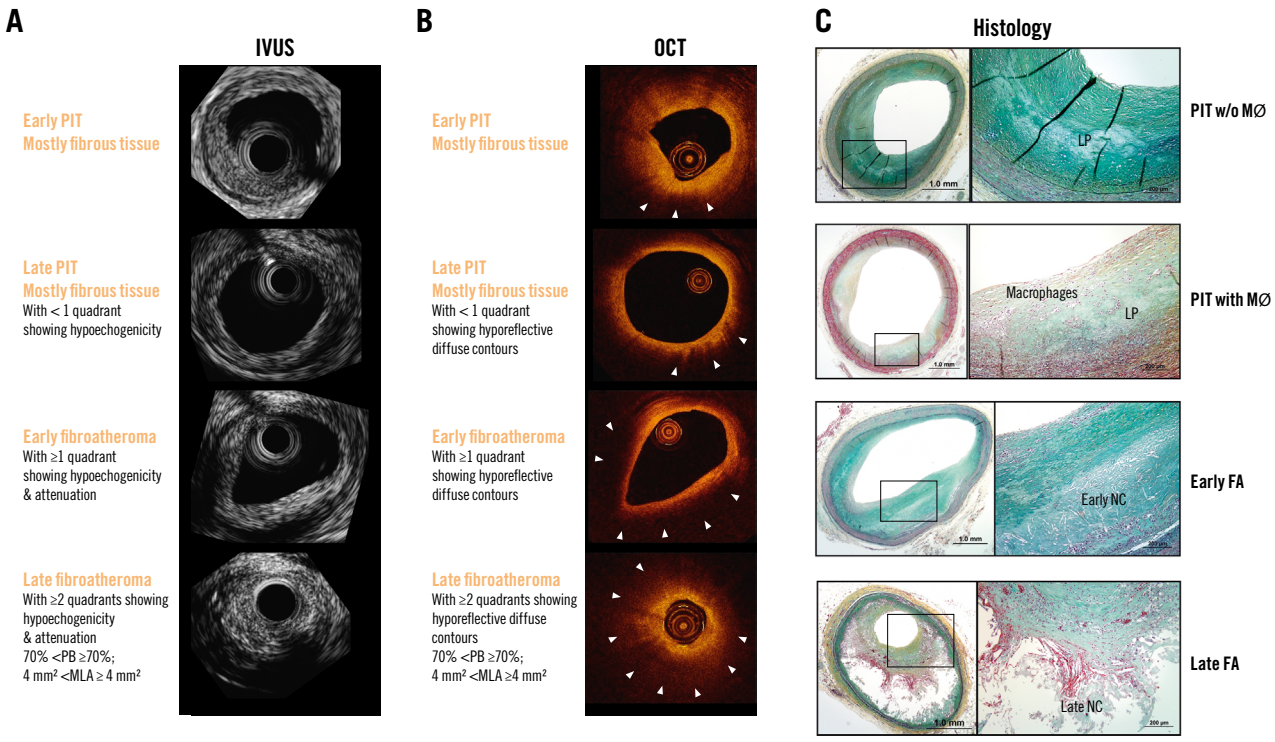

Figure 4. *Plaque types: revised nomenclature. Corresponding frames for IVUS (A), OCT (B), and histology (C). The top row shows a pathological intimal thickening plaque which is mostly normoechogenic by IVUS and hyperreflective by OCT. The second row also shows a pathological intimal thickening plaque which portrays more hypoechogenic tissue by IVUS and hyporeflective tissue with diffuse contours by OCT. OCT may show some macrophages, and therefore the "+" sign could be added to indicate the additional plaque characteristics. The third row depicts an early fibroatheroma with >1 quadrant of hypoechogenicity and attenuation by IVUS and by OCT, also with >1 quadrant of hyporeflective tissue with diffuse contours. The fourth row shows a late fibroatheroma plaque with high-risk plaque characteristics such as large plaque burden and reduced lumen area. (**Moving image 4**). Adapted with permission from*[101]*. FA: fibroatheroma; IVUS: intravascular ultrasound; LA: lumen area; LP: lipid pool; MØ: macrophages; MLA: minimum lumen area; NC: necrotic core; OCT: optical coherence tomography; PB: plaque burden; PIT: pathological intimal thickening*

Should imaging-verified high-risk plaques be treated mechanically with local devices regardless of physiological (functional) lesion severity?

In 2006, for the first time, it was demonstrated that plaque composition assessed by IVUS-integrated backscatter analysis was able to differentiate plaques that remained quiescent from those that progressed and caused events[38]; ever since, there have been numerous similar studies reported. In the PROSPECT study, 697 patients were included, all with an acute coronary syndrome (ACS) that had successful revascularisation and three-vessel VH-IVUS[7]. This study demonstrated that lesions with a small lumen area (<4 mm²), increased (>70%) plaque burden, and a TCFA phenotype were at risk of causing events[39]. The prognostic implications of a TCFA phenotype was also confirmed by the VIVA study[40], while the ATHEROREMO-IVUS[41] study showed that plaque burden and its phenotype, as assessed in a single vessel by VH-IVUS, provided useful prognostic information and was able to identify patients at risk of suffering a major adverse cardiovascular event (MACE)[40,41]. Taken altogether, these three studies showed that a large plaque burden (L1), plaque rich in lipid (L2), and plaque with a small residual minimum lumen area (L3) were associated with poor prognosis **(Figure 5, Moving image 5)**.

Despite the consistency of the data, the low positive predictive value of the VH-IVUS-derived plaque characteristics reported in these studies – range 18-24% – created scepticism about the potential clinical value of IVUS in stratifying cardiovascular risk and detecting high-risk plaques[42]. Due to these results, VH-IVUS use is decreasing in the clinical arena.

Subsequently, research focused on alternative intravascular imaging techniques such as NIRS-IVUS and OCT. The ATHEROREMO-NIRS study included 203 patients undergoing coronary catheterisation. It was found that patients with an increased lipid component (above the median) had a 4-fold increased risk of adverse cardiovascular events at 1-year follow-up[43]. Similarly, the Lipid Rich Plaque (LRP) study included 1,563 patients with suspected coronary artery disease who underwent invasive coronary angiography. NIRS-IVUS imaging in the non-culprit vessels showed that an increased max $LCBI_{4mm}$ was an independent predictor of MACE at patient- (hazard ratio [HR] 1.18, 95% confidence interval [CI]: 1.05-1.32; p=0.0043) and lesion-level analyses (HR 1.89, 95% CI: 1.26-2.83; p=0.0021)[2]. In line with these findings,

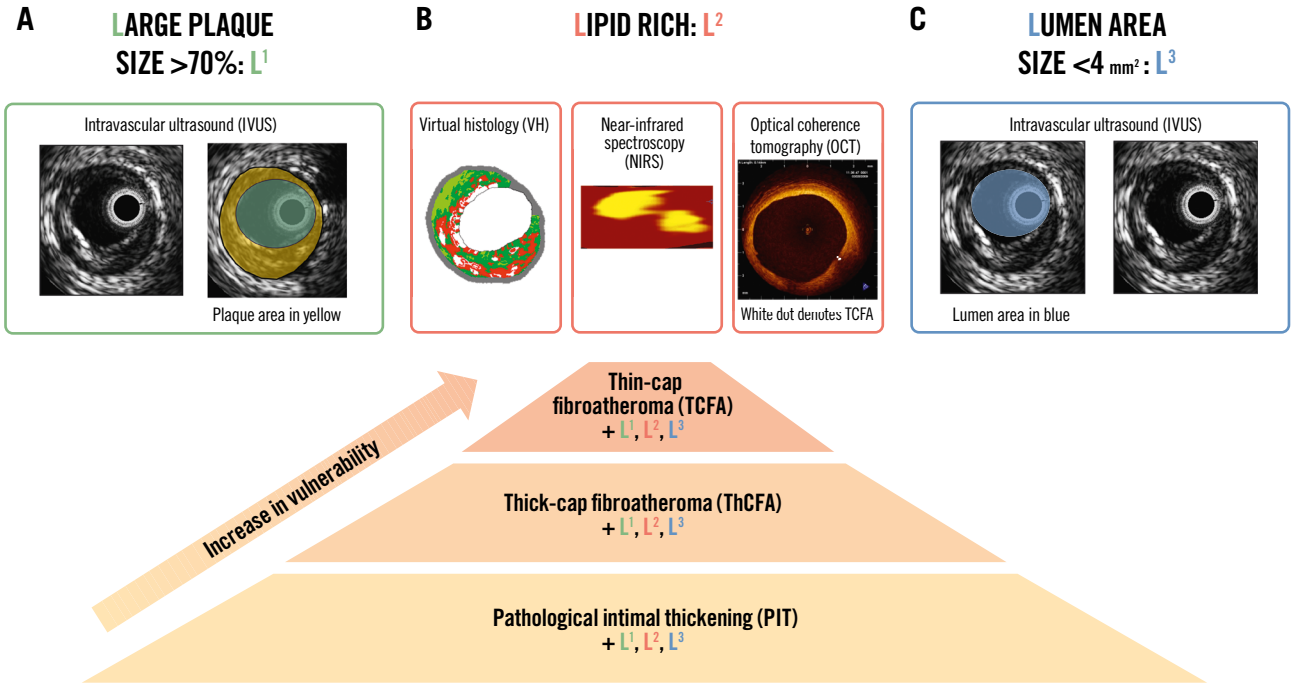

Figure 5. *Main high-risk plaque characteristics. A) Commonly found high-risk plaque characteristics include large plaque size >70% – also called L1. Note the plaque area shaded in yellow, which is usually reported in mm². Plaque size >70% is calculated as the ratio of the plaque area divided by the vessel area, which is called plaque burden. Secondly, the lipid (L2) content is also a marker of increased risk. As shown in* ***Figure 2****, there are many options for lipid characterisation. Lastly, a luminal (L3) area less than 4 mm² is also associated with poor long-term outcomes. These L1, L2, and L3 plaque characteristics in addition to the PIT, TCFA and ThCFA should be reported. For example, a TCFA+L1+L2+L3 means that it is a TCFA whose plaque size is >70%, lipid content is large, and minimum lumen area is >4 mm². B) It has been proposed that vulnerability increases from PIT through ThCFA to TCFA. (****Moving image 5****).*

the PROSPECT II study[44] recruited 898 patients admitted with an ACS who had undergone successful revascularisation and NIRS-IVUS imaging in the non-culprit vessels; these patients were followed up for 3.7 years. During this period, 66 events were reported that were caused from 78 non-culprit lesions; lesions with a large lipid core and increased plaque burden were at a high risk of causing these events (7.0%, 95% CI: 4.0-10.0). Patients with these lesions had a 4-year non-culprit lesion-related MACE rate of 13.2% (95% CI: 9.4-17.6).

Finally, two prospective OCT-based imaging studies have confirmed the value of this imaging modality in stratifying risk. In the CLIMA study, 1,003 patients who had been referred for an invasive assessment of the coronary artery anatomy underwent OCT imaging in the left anterior descending coronary artery and were followed up for 1 year. A minimum lumen area <3.5 mm², the presence of a lipid arc greater than 180 degrees, a thin fibrous cap <75 µm, and the presence of macrophages were associated with a higher incidence of cardiac death or target vessel myocardial infarction. Patients having lesions with all of the above plaque characteristics had an increased risk, with an 18.9% event rate at 1-year follow-up[45].

Similarly, in the COMBINE OCT-FFR study that included 390 diabetic patients with intermediate non-flow-limiting lesions assessed by fractional flow reserve (FFR), OCT showed that lesions with a TCFA phenotype were more likely to cause MACE than lesions with different plaque morphologies (13.3% vs 3.1%; p<0.001)[46]. These findings were also confirmed in a three-vessel OCT imaging study including 883 patients with an acute myocardial infarction (AMI) that underwent successful revascularisation. In this report, a TCFA phenotype (adjusted HR 8.15, 95% CI: 3.67-18.07) and a minimum lumen area <3.5 mm² (adjusted HR 4.33, 95% CI: 1.81-10.38) were found to be independent predictors of non-culprit lesion-related MACE[47].

There have been few studies evaluating local treatment of lesions that portray high-risk plaque characteristics. The SECRITT trial enrolled 23 patients who met the enrolment criteria (presence of non-obstructive VH-derived TCFA lesion with a thin cap on OCT) and were randomised to vShield (n=13; Prescient Medical) versus medical therapy (n=10). vShield is a nitinol self-expanding device which was associated with no device-related MACE at 6-month follow-up[48]. Then, the PROSPECT ABSORB study randomised patients with an angiographically non-obstructive stenosis that was not intended for PCI but had an IVUS plaque burden of ≥65% to receive a bioresorbable vascular scaffold (BVS) plus guideline-directed medical therapy (GDMT) versus GDMT alone. The primary endpoint, minimum lumen area, was larger in the

BVS group, at 6.9 mm^2 compared with 3.0 mm^2 in lesions treated with GDMT only. A relevant, hypothesis-generating finding was that MACE occurred in 4.3% of BVS-treated patients versus 10.7% of GDMT-only patients at follow-up[49].

The PREVENT trial[8] included patients with non-flow-limiting (FFR >0.80) vulnerable coronary plaques identified by intracoronary imaging. Patients were randomly assigned (1:1) to either PCI plus optimal medical therapy or optimal medical therapy alone. Vulnerability was defined as having 2 of the following 4 characteristics: a minimum lumen area <4.0 mm^2 by IVUS or OCT, a plaque burden of more than 70% by IVUS, a lipid-rich plaque by NIRS (max $LCBI_{4mm}$ >315), or a thin-cap fibroatheroma detected by VH-IVUS (defined as a ≥10% confluent necrotic core with >30° abutting the lumen in three consecutive frames on VH-IVUS) or by OCT (defined as a lipid plaque with arc >90° and fibrous cap thickness <65 µm). Most patients had plaque burden (PB) and minimum lumen area as qualifying criteria. At 2 years, target vessel failure (the primary outcome) occurred in 3 (0.4%) patients in the preventive percutaneous coronary intervention group and in 27 (3.4%) patients in the optimal medical therapy group (absolute difference –3.0 percentage points [95% CI: –4.4 to –1.8]; p=0.0003). The authors concluded, "The PREVENT study findings support an expansion of the indications for percutaneous coronary intervention to include non-flow-limiting, high-risk, vulnerable plaques." However, information as to whether the events during follow-up were related to the randomised plaques has not been provided yet. To effectively translate these results into clinical practice would require that all patients undergo three-vessel FFR and invasive imaging, which are not widely available. Previous studies also showed that invasive imaging does not reach every segment in the coronary tree, and often the MACE that arise during follow-up come from non-imaged lesions. Therefore, CCTA (plus CT-derived FFR) could be an excellent screening tool to target vessels more efficiently for FFR and invasive imaging.

In addition, several prospective randomised studies (e.g., INTERCLIMA [ClinicalTrials.gov: NCT05027984], COMBINE-INTERVENE [NCT05333068], and VULNERABLE [NCT05599061]) are exploring the prognostic benefit of a pre-emptive invasive treatment of high-risk but non-flow-limiting lesions detected by intravascular imaging.

Thus, in summary, plaques with high-risk features are those that in the follow-up have been associated with MACE, although, overall, their positive predictive value remains low. The imaging variable that is most consistently related with long-term cardiovascular complications is a large plaque burden (L1, PB >70%); additionally, lipid-rich content (L2) with or without TCFA and a small residual lumen area (L3, <4 mm^2) have been also found to be associated with long-term cardiovascular outcomes. Whether these plaques should be pre-emptively treated with local devices is currently being explored in the above-mentioned studies.

Should culprit plaques be imaged with intravascular imaging before stenting to tailor therapy?

PLAQUE RUPTURE

PR of infarct-related or target lesions occurred in 66% of AMI patients and in 27% of stable angina (SA) patients. Non-infarct-related or non-target artery PR occurred in 17% of AMI patients and 5% of SA patients. Multiple PRs were observed in 20% of AMI patients and 6% of SA patients[50].

Other reports showed similar findings[51]. In the context of AMI, PRs are treated locally, in the infarct-related artery, with drug-eluting stents (DES) or drug-eluting balloons. The former is the current standard of care, and the latter technology is building promising evidence but remains to be further established[52-57]. Yet, the additional plaque ruptures do not require any local treatment since they heal over time and do not seem to portend a risk of future events.

Niccoli et al[58] showed that preintervention OCT image analysis before DES implantation was prognostically relevant. At follow-up, adverse events occurred more frequently (39% vs 14%; p<0.001) in patients in whom thrombotic culprit lesions showed PR versus plaques with an intact surface. This was mainly driven by a higher risk of unstable angina and target vessel revascularisation. The authors suggested that the presence of a PR at the culprit lesion portends a poor prognosis even in patients successfully treated with DES and, therefore, that this information might be used to risk stratify and manage ACS patients.

PLAQUE EROSION

Intravascular imaging is providing insights as to whether ACS without fibrous cap disruption could be treated without stenting. Although there is not yet a final position on this, we present below the evidence that is being considered in this regard.

In the Massachusetts General Hospital OCT Registry[59], 31% of patients had PE as detected by OCT. Patients with OCT-detected erosion were younger, had less severe stenosis, less thrombus burden, and less frequently presented with ST-segment elevation myocardial infarction (STEMI) than those with plaque rupture. Non-STEMI (NSTEMI) was the predominant presentation in patients with OCT-detected erosion.

Prati et al[60] suggested that, in patients with ACS without severe residual lumen narrowing and an intact fibrous cap visualised on OCT, an intense antithrombotic strategy alone (without coronary stenting) was able to provide excellent long-term clinical outcomes. They initially reported the clinical outcomes of 12 out of 31 STEMI patients with an intact fibrous cap managed with thrombectomy and dual antiplatelet therapy alone (without stent implantation). Notably, after 2-year follow-up, none of these patients required coronary revascularisation. These investigators first proposed that, in patients with non-severe lesions after thrombus aspiration, this conservative management ("with a thromboaspiration-alone strategy") would allow vessel wall healing and complete restoration of the endothelial lining.

Further, the EROSION study confirmed that, in selected patients with ACS caused by PE, a novel strategy of antithrombotic therapy alone with aspirin and ticagrelor (but without stenting) provided favourable 1-month clinical outcomes[61]. Among 405 ACS patients (97% with STEMI) with analysable OCT images, PE was found in 103 of them (25%). Most patients were treated acutely with tirofiban and thrombus aspiration. Once stabilised, patients showing normal coronary flow and <70% residual diameter stenosis at the culprit lesion were treated with the dual antiplatelet

strategy alone. Sixty patients were eventually enrolled, and 55 of them were re-evaluated with OCT at 1 month. The primary endpoint of the EROSION study, a >50% reduction in thrombus volume at 1 month, was met in 47/60 patients (78%), and no trace of residual thrombus was visualised in 22 patients. The favourable long-term clinical results obtained by this strategy were also subsequently demonstrated. Residual thrombus volume further decreased from 1 month to 1 year (0.3 mm^3 vs 0.1 mm^3; p=0.001) with no visible residual thrombus in half of the patients and, from a clinical standpoint, 92.5% of patients remained event-free at 1 year[62].

The EROSION III study is the first randomised clinical trial in this field. Patients with STEMI, angiographic diameter stenosis ≤70% and Thrombolysis in Myocardial Infarction (TIMI) flow grade 3 (at presentation or after antegrade blood flow restoration) were randomised (n=246) to either OCT guidance or angiographic guidance. Notably, both patients with OCT-detected PE and those showing small PR were included. The primary efficacy (surrogate) endpoint, the rate of stent implantation, was significantly lower in the OCT arm (44% vs 59%; p<0.05). In addition, the rates of cardiocerebrovascular events were comparable between the groups (11.6% after OCT guidance vs 9.6% after angiographic guidance; p=0.66), although this study was not powered for a comparison of clinical event rates at 1 year[63].

Thus, despite the evidence in this section suggesting that patients with plaque erosion could be treated differently, compared to those with plaque rupture, the level of evidence is not yet sufficient to inform a change in clinical practice.

ERUPTIVE CALCIFIED NODULES

Eruptive CNs are present in a minority (~5-10%) of ACS patients. Importantly, results of coronary interventions in CNs or nodular calcifications are poorer than the outcomes found in other types of calcified plaques[59,64]. In some cases, results are clearly suboptimal despite the aggressive use of calcium modification techniques (including scoring and very high-pressure balloons, rotational or orbital atherectomy, and lithotripsy) **(Figure 3, Moving image 3)**.

Some culprit lesions of ACS patients may not fit into this uniform, classical algorithm (namely, plaque rupture, erosion, or calcified nodules). Other potential aetiologies, including superficial calcific sheets, have emerged. Clinical reports showed that patients with ACS who have calcification in the culprit lesions have a worse prognosis[65,66]. Anecdotal preliminary OCT reports have already suggested that superficial calcific sheets could indeed generate atherothrombotic complications leading to an ACS[67].

In a multicentre study of 1,241 ACS patients with preintervention OCT available, 157 patients (12.7%) had a calcified plaque (defined in this study as superficial calcification without images of a ruptured lipid plaque) at the culprit lesion. Three distinct types of culprit calcified plaque were considered: (1) superficial calcific sheet (67.4%), (2) typical eruptive calcified nodules (25.5%), and (3) calcified protrusions (7.1%). The eruptive CNs were more frequently located in the right coronary artery, whereas the superficial calcific sheets were more frequently found in the left anterior descending coronary artery. The superficial calcific sheets had the most severe lumen narrowing and the worst coronary flow. Of interest, among 95 patients with a superficial calcific sheet, 81 (85%) showed "minimally disrupted" overlying fibrous tissue and the highest rise in cardiac biomarkers after stenting. Furthermore, white thrombus was predominant in this group, whereas most eruptive calcified nodules showed associated red thrombus[68]. The pathophysiology of a superficial calcific sheet to produce ACS remains elusive, and histological validation of superficial calcific sheets as the cause of ACS is eagerly awaited.

Assessment of the impact of medical treatment on atherosclerosis progression

IVUS has been the intracoronary imaging modality of choice to study the changes in plaque (percentage atheroma volume is the most used endpoint) by lowering the low-density lipoprotein cholesterol (LDL-C) plasma concentration; IVUS has also historically been used to compare the various antiatherosclerotic strategies[69]. The most contemporary trials also have used CCTA, OCT, or a multimodality imaging approach including IVUS, OCT, and NIRS[70]. Thereby, newer endpoints have been developed, such as lipid composition measured by different metrics, including lipid arc by OCT and lipid core burden index by NIRS, while in CCTA, a combination of plaque geometric and compositional endpoints have been used.

IVUS TRIALS

Selected IVUS studies showing the stabilisation and regression of atherosclerotic plaques are included in **Table 1**.

ANTILIPID THERAPIES

Statin trials have evaluated different statin types and dose regimens. In the REVERSAL trial, high-intensity atorvastatin led to significant plaque regression[71]. The ASTEROID study demonstrated for the first time that high-dose rosuvastatin had plaque-regression capabilities[72]. A head-to-head comparison of atorvastatin and rosuvastatin was reported in the SATURN trial[73]. Although rosuvastatin lowers more LDL-C, the extent of plaque regression was of a similar magnitude in both study arms. When statins alone do not achieve the recommended targets, ezetimibe has been used in combination. This combination did not exert additional plaque-regression effects in the primary endpoints of the HEAVEN, ZEUS, PRECISE-IVUS, and EZETIMIBE-ACS trials[74-77]. Despite its value, the amount of plaque regression achieved by aggressive statin therapy remains very low (<1%).

Proprotein convertase subtilisin/kexin type 9 (PCSK9) inhibitors are monoclonal antibodies (evolocumab and alirocumab) that target the PCSK9 enzyme. The GLAGOV trial showed that evolocumab in addition to statin versus statin/placebo induced plaque regression[78]. Similarly, in the HUYGENS trial, evolocumab consistently showed reduction in plaque size[79].

In the PACMAN-AMI trial, alirocumab showed plaque regression in non-infarct-related arteries[70], while in the ODYSSEY J-IVUS trial, a reduced dose of alirocumab did not reach statistical significance versus placebo in terms of plaque regression[80].

Other antilipid therapies such as cholesterol ester transfer protein inhibitors (torcetrapib) and a triglyceride-lowering agent (eicosapentaenoic acid) did not demonstrate an effect on plaque size.

Table 1. Coronary plaque stabilisation and regression studies: IVUS imaging.

Statin trials	Reference	Primary endpoint	Results
REVERSAL (R) atorvastatin 80 mg vs pravastatin 40 mg	71	PAV	At 18 months, atorvastatin reduced progression
ASTEROID (NR) rosuvastatin 40 mg	72	Change in PAV and the change in nominal atheroma volume in the 10 mm subsegment	At 24 months, rosuvastatin induced significant regression
SATURN (R) atorvastatin 80 mg vs rosuvastatin 40 mg	73	PAV	At 24 months, both drugs induced significant (& similar) regression
COSMOS (NR) rosuvastatin 2.5 mg titrated to 20 mg	94	Percentage change in plaque volume	At 18 months, rosuvastatin induced significant regression
IBIS-4 (NR) rosuvastatin 40 mg	91,93	PAV	At 13 months, rosuvastatin induced significant regression
STABLE (R) rosuvastatin 40 mg vs 10 mg	95	Virtual histology-defined percentage compositional volume	At 12 months, rosuvastatin reduced necrotic core and plaque volume
JAPAN-ACS (R) pitavastatin 4 mg or atorvastatin 20 mg	96	Mean percentage change in PV	At 8-12 months, both drugs induced significant (& similar) regression
PCSK9 inhibitor trials			
GLAGOV (R) evolocumab 420 mg vs placebo	78	PAV	At 18 months, evolocumab induced significant regression
HUYGENS (R) evolocumab 420 mg vs placebo	79	PAV (secondary endpoint)	At 12 months, evolocumab induced significant regression
PACMAN-AMI (R) alirocumab 150 mg vs placebo	70	PAV	At 12 months, alirocumab induced significant regression
ODYSSEY-J-IVUS (R) alirocumab 75 mg vs placebo	80	Percentage change in normalised total atheroma volume	At 36 weeks, the effect of alirocumab did not reach statistical significance
Cholesterol ester transfer protein inhibitors			
ILLUSTRATE (R) torcetrapib plus atorvastatin vs atorvastatin alone	97	PAV	At 24 months, no effect of torcetrapib addition on PAV
Triglyceride-lowering agent			
CHERRY (R) eicosapentaenoic acid 1,800 mg plus pitavastatin 4 mg vs pitavastatin 4 mg	98	Plaque volume and composition	At 6-8 months, no difference in PAV between groups
HDL-C mimetics			
CHI SQUARE (R) placebo vs CER-001 3 mg/kg, 6 mg/kg, or 12 mg/kg	99	Nominal change in the total atheroma volume	At ~9 weeks, CER-001 infusions did not reduce plaque
CER-001 Atherosclerosis Regression Acute Coronary Syndrome (R) CER-001 3 mg/kg vs placebo	100	PAV	At 78 days, CER-001 did not promote regression
ApoA-I Milano (R) placebo vs ETC-216 15 mg/kg vs 45 mg/kg	82	PAV	At ~7 weeks, ApoA-I Milano/phospholipid complex (ETC-216) produced significant regression
Thiazolidinediones			
PERISCOPE (R) glimepiride 1-4 mg vs pioglitazone 15-45 mg	84	PAV	At 18 months, pioglitazone slowed progression of plaques
APPROACH (R) rosiglitazone 4 mg/d vs glipizide 5 mg/d	85	PAV	At 18 months, rosiglitazone showed mild plaque regression, but it did not affect plaque size more than glipizide
Antihypertensive drugs			
CAMELOT (R) amlodipine 10 mg vs enalapril 20 mg vs placebo	86	PAV	At 24 months, amlodipine showed a non-significant trend towards less progression of plaque, while enalapril and placebo showed progression
PERSPECTIVE (R) perindopril 8 mg vs placebo	87	Mean plaque cross-sectional area	At 3 years, perindopril did not change plaque size
OLIVUS (R) olmesartan 10-40 mg vs control	88	PAV	At 14 months, olmesartan decreased plaque size

HDL-C: high-density lipoprotein cholesterol; IVUS: intravascular ultrasound; NR: non-randomised; PAV: percentage atheroma volume; PCSK9: proprotein convertase subtilisin/kexin type 9; PV: plaque volume; R: randomised

High-density lipoprotein (HDL) cholesterol mimetics, which aim at increasing HDL levels, have shown conflicting results from their inception. Recombinant apolipoprotein A-I Milano (ApoA-IM) dimer showed a reduction of carotid intimal thickening in rabbits[81]. This was followed by a successful IVUS study by Nissen et al, who showed that an ApoA-I Milano/phospholipid complex (ETC-216) produced significant regression[82]. Conversely, CER-001 showed no effects on plaque size, and lastly, CSL112, which is a human apolipoprotein A1, was evaluated in the AEGIS-II study and resulted in no reduction of cardiovascular outcomes[83].

NON-LIPID TARGETS

Thiazolidinediones are medications for treating type 2 diabetes mellitus. In the PERISCOPE trial[84], pioglitazone reduced plaque size, while in the APPROACH trial[85], rosiglitazone did not affect plaque size more than glipizide.

Antihypertensive drugs have shown conflicting results in terms of their effects on coronary plaques. In the CAMELOT trial, amlodipine, enalapril and placebo were compared. Amlodipine showed regression of plaque, albeit non-significant, while the other two groups showed its progression[86]. The PERSPECTIVE trial did not show plaque reduction in the perindopril group[87]. Conversely, olmesartan decreased plaque size in the OLIVUS trial[88]. Lastly, the AQUARIUS trial did not show beneficial effects with the use of aliskiren[89].

OCT TRIALS

OCT is unable to visualise the entire plaque burden in segments with advanced CAD. Therefore, OCT primary study endpoints have been lipid arc and fibrous cap thickness, given the excellent resolution of OCT.

ANTILIPID THERAPIES

A systematic review and meta-analysis that pooled the results of 9 statin trials showed that FCT increased by 67.7 µm with statin therapy[90]. Trials not included in this meta-analysis are summarised below.

IBIS-4 was a prospective observational study in 103 patients presenting with STEMI. IVUS and OCT were performed in 2 non-infarct-related arteries at baseline presentation in order to then assess the effect of rosuvastatin 40 mg on fibrous cap thickness and macrophage line arc by OCT at 13-month follow-up. The study showed a significant increase in FCT from 64.9±19.9 µm to 87.9±38.1 µm (p=0.008) and a reduction in macrophage line arc from 9.6±12.8° to 6.4±9.6° (p<0.0001); further, 69.2% of TCFAs identified at baseline regressed to a non-TCFA morphology[91].

PCSK9 INHIBITORS

The ALTAIR trial was a prospective, randomised, single-centre study that included 24 patients undergoing stent implantation. Patients were randomised to receive either alirocumab 75 mg every 2 weeks plus rosuvastatin 10 mg or to rosuvastatin 10 mg alone, to assess the effect of adding the PCSK9 inhibitor alirocumab to rosuvastatin in patients with TCFA who underwent coronary stent implantation. It showed a significant increase in FCT (140 µm vs 45 µm; p=0.002), a significant decrease in lipid index (–26.2% vs –2.8%; p<0.001) and a decrease in macrophage grade (–28.4% vs –10.2%; p=0.033)[92].

The HUYGENS trial was a prospective and randomised trial in 161 patients presenting with NSTEMI who underwent OCT and IVUS imaging of non-culprit vessels at baseline and at 50 weeks post-presentation. Patients were randomised to either evolocumab 420 mg or placebo every month while taking the maximum tolerated statin dose, to assess the change in the minimum FCT and maximum lipid arc. It showed a greater increase in the minimum FCT (42.7 µm vs 21.5 µm; p=0.015) and a decrease in the maximum lipid arc (–57.5° vs –31.4°; p=0.04) and macrophage index (–3.17 mm vs –1.45 mm; p=0.04)[79].

The PACMAN-AMI trial was a prospective and randomised trial in 300 patients presenting with STEMI or NSTEMI who underwent IVUS, NIRS, and OCT imaging of non-culprit vessels at baseline and at 52 weeks. Patients were randomised to either alirocumab 150 mg every 2 weeks or placebo while taking rosuvastatin 20 mg, to assess the change in IVUS-derived percentage atheroma, in NIRS-derived max $LCBI_{4mm}$, and in OCT-derived minimum FCT from baseline to week 52. It showed a greater increase in the minimum FCT (62.67 µm vs 33.19 µm; p=0.001); other parameters have been described before[70].

The YELLOW III trial was a prospective observational trial in 137 patients undergoing percutaneous interventions who had a non-obstructive, non-culprit lesion with luminal stenosis 30-50%; these patients underwent OCT and NIRS/IVUS imaging at baseline and at 26 weeks. Patients were randomised to either evolocumab 420 mg or placebo every month while taking the maximum tolerated statin dose, to assess the change in max $LCBI_{4mm}$ by NIRS/IVUS and OCT-derived FCT from baseline to week 26. It showed a significant increase in the minimum FCT (97.7±31.1 µm to 70.9±21.7 µm; p<0.001) and a significant decrease in both maximum lipid arc (189.1±73.4° to 161.6±68.7°; p<0.001) and maximum macrophage arc (122.1±67.7° to 148.2±72.5°; p<0.0001) (ClinicalTrials.gov: NCT04710368; unpublished as of yet).

Conclusions

In conclusion, intravascular imaging has positively impacted how we evaluate coronary atherosclerosis and its natural history; it also provides guidance on the use of tailored therapies and enables the assessment of their long-term follow-up effects.

Authors' affiliations

1. Interventional Cardiology, MedStar Washington Hospital Center, Washington, D.C., USA; 2. Hospital Universitari i Politecnic La Fe, Valencia, Spain; 3. Centro de Investigación Biomedica en Red (CIBERCV) – Madrid, Madrid, Spain; 4. Department of Medicine, Division of Cardiology, McMaster University, Hamilton, ON, Canada; 5. Population Health Research Institute, Hamilton, ON, Canada; 6. National Laboratory for Scientific Computing, Petrópolis, Brazil; 7. Department of Cardiology, Barts Heart Centre, Barts Health NHS Trust, London, United Kingdom; 8. Cardiovascular Devices Hub, Centre for Cardiovascular Medicine and Devices, William Harvey Research Institute,

Queen Mary University of London, London, United Kingdom; 9. Department of Cardiology, Hospital Universitario de La Princesa, IIS-IP, CIBERCV, Universidad Autónoma de Madrid, Madrid, Spain

Conflict of interest statement

H.M. Garcia-Garcia has grants or contracts from Medtronic, Biotronik, Abbott, Neovasc, Corflow, Lucent Bio, Philips, and Chiesi (paid to the institution); and received consulting fees from Boston Scientific, Medis, Abbott, and ACIST. N. Pinilla-Echeverri has served as a consultant and speaker, received research grant support, and served on the advisory board for Abbott; has served on the advisory board for Philips; and has served as a consultant for Conavi, Amgen, Bayer, and Novartis. The other authors have no conflicts of interest to declare.

References

1. Virchow R. Cellular pathology. As based upon physiological and pathological histology. Lecture XVI--Atheromatous affection of arteries. 1858. *Nutr Rev*. 1989;47:23-5.
2. Waksman R, Di Mario C, Torguson R, Ali ZA, Singh V, Skinner WH, Artis AK, Cate TT, Powers E, Kim C, Regar E, Wong SC, Lewis S, Wykrzykowska J, Dube S, Kazziha S, van der Ent M, Shah P, Craig PE, Zou Q, Kolm P, Brewer HB, Garcia-Garcia HM; LRP Investigators. Identification of patients and plaques vulnerable to future coronary events with near-infrared spectroscopy intravascular ultrasound imaging: a prospective, cohort study. *Lancet*. 2019;394:1629-37.
3. Pu J, Mintz GS, Biro S, Lee JB, Sum ST, Madden SP, Burke AP, Zhang P, He B, Goldstein JA, Stone GW, Muller JE, Virmani R, Maehara A. Insights into echo-attenuated plaques, echolucent plaques, and plaques with spotty calcification: novel findings from comparisons among intravascular ultrasound, near-infrared spectroscopy, and pathological histology in 2,294 human coronary artery segments. *J Am Coll Cardiol*. 2014;63:2220-33.
4. Nishimura RA, Edwards WD, Warnes CA, Reeder GS, Holmes DR Jr, Tajik AJ, Yock PG. Intravascular ultrasound imaging: in vitro validation and pathologic correlation. *J Am Coll Cardiol*. 1990;16:145-54.
5. Potkin BN, Bartorelli AL, Gessert JM, Neville RF, Almagor Y, Roberts WC, Leon MB. Coronary artery imaging with intravascular high-frequency ultrasound. *Circulation*. 1990;81:1575-85.
6. Gonzalo N, García-García HM, Ligthart J, Rodriguez-Granillo G, Meliga E, Onuma Y, Schuurbiers JC, Bruining N, Serruys PW. Coronary plaque composition as assessed by greyscale intravascular ultrasound and radiofrequency spectral data analysis. *Int J Cardiovasc Imaging*. 2008;24:811-8.
7. García-García HM, Mintz GS, Lerman A, Vince DG, Margolis MP, van Es GA, Morel MA, Nair A, Virmani R, Burke AP, Stone GW, Serruys PW. Tissue characterisation using intravascular radiofrequency data analysis: recommendations for acquisition, analysis, interpretation and reporting. *EuroIntervention*. 2009;5:177-89.
8. Park SJ, Ahn JM, Kang DY, Yun SC, Ahn YK, Kim WJ, Nam CW, Jeong JO, Chae IH, Shiomi H, Kao HL, Hahn JY, Her SH, Lee BK, Ahn TH, Chang KY, Chae JK, Smyth D, Mintz GS, Stone GW, Park DW; PREVENT Investigators. Preventive percutaneous coronary intervention versus optimal medical therapy alone for the treatment of vulnerable atherosclerotic coronary plaques (PREVENT): a multicentre, open-label, randomised controlled trial. *Lancet*. 2024;403:1753-65.
9. Tearney GJ, Regar E, Akasaka T, Adriaenssens T, Barlis P, Bezerra HG, Bouma B, Bruining N, Cho JM, Chowdhary S, Costa MA, de Silva R, Dijkstra J, Di Mario C, Dudek D, Falk E, Feldman MD, Fitzgerald P, Garcia-Garcia HM, Gonzalo N, Granada JF, Guagliumi G, Holm NR, Honda Y, Ikeno F, Kawasaki M, Kochman J, Koltowski L, Kubo T, Kume T, Kyono H, Lam CC, Lamouche G, Lee DP, Leon MB, Maehara A, Manfrini O, Mintz GS, Mizuno K, Morel MA, Nadkarni S, Okura H, Otake H, Pietrasik A, Prati F, Räber L, Radu MD, Rieber J, Riga M, Rollins A, Rosenberg M, Sirbu V, Serruys PW, Shimada K, Shinke T, Shite J, Siegel E, Sonoda S, Suter M, Takarada S, Tanaka A, Terashima M, Thim T, Uemura S, Ughi GJ, van Beusekom HM, van der Steen AF, van Es GA, van Soest G, Virmani R, Waxman S, Weissman NJ, Weisz G; International Working Group for Intravascular Optical Coherence Tomography (IWG-IVOCT). Consensus standards for acquisition, measurement, and reporting of intravascular optical coherence tomography studies: a report from the International Working Group for Intravascular Optical Coherence Tomography Standardization and Validation. *J Am Coll Cardiol*. 2012;59:1058-72.
10. Benedek T, Jako B, Benedek I. Plaque quantification by coronary CT and intravascular ultrasound identifies a low CT density core as a marker of plaque instability in acute coronary syndromes. *Int Heart J*. 2014;55:22-8.
11. Marwan M, Taher MA, El Meniawy K, Awadallah H, Pflederer T, Schuhbäck A, Ropers D, Daniel WG, Achenbach S. In vivo CT detection of lipid-rich coronary artery atherosclerotic plaques using quantitative histogram analysis: a head to head comparison with IVUS. *Atherosclerosis*. 2011;215:110-5.
12. Ramasamy A, Parasa R, Sokooti H, Zhang X, Tanboga IH, Kitslaar P, Broersen A, Rathod KS, Amersey R, Jain A, Ozkor M, Reiber JHC, Dijkstra J, Serruys PW, Moon JC, Mathur A, Torii R, Pugliese F, Baumbach A, Bourantas CV. Computed tomography versus near-infrared spectroscopy for the assessment of coronary atherosclerosis. *EuroIntervention*. 2024;20:e1465-e1475.
13. Mintz GS. Intravascular imaging of coronary calcification and its clinical implications. *JACC Cardiovasc Imaging*. 2015;8:461-71
14. Friedrich GJ, Moes NY, Mühlberger VA, Gabl C, Mikuz G, Hausmann D, Fitzgerald PJ, Yock PG. Detection of intralesional calcium by intracoronary ultrasound depends on the histologic pattern. *Am Heart J*. 1994;128:435-41
15. Wang X, Matsumura M, Mintz GS, Lee T, Zhang W, Cao Y, Fujino A, Lin Y, Usui E, Kanaji Y, Murai T, Yonetsu T, Kakuta T, Maehara A. In Vivo Calcium Detection by Comparing Optical Coherence Tomography, Intravascular Ultrasound, and Angiography. *JACC Cardiovasc Imaging*. 2017;10:869-79.
16. Mehanna E, Bezerra HG, Prabhu D, Brandt E, Chamié D, Yamamoto H, Attizzani GF, Tahara S, Van Ditzhuijzen N, Fujino Y, Kanaya T, Stefano G, Wang W, Gargesha M, Wilson D, Costa MA. Volumetric characterization of human coronary calcification by frequency-domain optical coherence tomography. *Circ J*. 2013;77:2334-40.
17. Prati F, Gatto L, Fabbiocchi F, Vergallo R, Paoletti G, Ruscica G, Marco V, Romagnoli E, Boi A, Fineschi M, Calligaris G, Tamburino C, Crea F, Ozaki Y, Alfonso F, Arbustini E. Clinical outcomes of calcified nodules detected by optical coherence tomography: a sub-analysis of the CLIMA study. *EuroIntervention*. 2020;16:380-6.
18. Fujino A, Mintz GS, Matsumura M, Lee T, Kim SY, Hoshino M, Usui E, Yonetsu T, Haag ES, Shlofmitz RA, Kakuta T, Maehara A. A new optical coherence tomography-based calcium scoring system to predict stent underexpansion. *EuroIntervention*. 2018;13:e2182-9.
19. Zhang M, Matsumura M, Usui E, Noguchi M, Fujimura T, Fall KN, Zhang Z, Nazif TM, Parikh SA, Rabbani LE, Kirtane AJ, Collins MB, Leon MB, Moses JW, Karmpaliotis D, Ali ZA, Mintz GS, Maehara A. Intravascular Ultrasound-Derived Calcium Score to Predict Stent Expansion in Severely Calcified Lesions. *Circ Cardiovasc Interv*. 2021;14:e010296.
20. Garcia-Garcia HM, Sanz-Sánchez J. Call to ACTION: Coronary Calcium Needs Comprehensive Evaluation and Preparation. *JACC Cardiovasc Interv*. 2025;18:634-36.
21. Youssef G, Kalia N, Darabian S, Budoff MJ. Coronary calcium: new insights, recent data, and clinical role. *Curr Cardiol Rep*. 2013;15:325.
22. Maurovich-Horvat P, Ferencik M, Voros S, Merkely B, Hoffmann U. Comprehensive plaque assessment by coronary CT angiography. *Nat Rev Cardiol*. 2014;11:390-402.
23. Nieman K, García-García HM, Hideo-Kajita A, Collet C, Dey D, Pugliese F, Weissman G, Tijssen JGP, Leipsic J, Opolski MP, Ferencik M, Lu MT, Williams MC, Bruining N, Blanco PJ, Maurovich-Horvat P, Achenbach S. Standards for quantitative assessments by coronary computed tomography angiography (CCTA): An expert consensus document of the society of

cardiovascular computed tomography (SCCT). *J Cardiovasc Comput Tomogr.* 2024;18:429-43.

24. van Velzen JE, de Graaf FR, de Graaf MA, Schuijf JD, Kroft LJ, de Roos A, Reiber JH, Bax JJ, Jukema JW, Boersma E, Schalij MJ, van der Wall EE. Comprehensive assessment of spotty calcifications on computed tomography angiography: comparison to plaque characteristics on intravascular ultrasound with radiofrequency backscatter analysis. *J Nucl Cardiol.* 2011;18:893-903.

25. Chu M, Jia H, Gutiérrez-Chico JL, Maehara A, Ali ZA, Zeng X, He L, Zhao C, Matsumura M, Wu P, Zeng M, Kubo T, Xu B, Chen L, Yu B, Mintz GS, Wijns W, Holm NR, Tu S. Artificial intelligence and optical coherence tomography for the automatic characterisation of human atherosclerotic plaques. *EuroIntervention.* 2021;17:41-50.

26. Garg M, Garcia-Garcia HM, Calderón AT, Gupta J, Sortur S, Levine MB, Singla P, Picchi A, Sardella G, Adamo M, Frigoli E, Limbruno U, Rigattieri S, Diletti R, Boccuzzi G, Zimarino M, Contarini M, Russo F, Calabro P, Andò G, Varbella F, Garducci S, Palmieri C, Briguori C, Sánchez JS, Valgimigli M. Reproducibility of an artificial intelligence optical coherence tomography software for tissue characterization: Implications for the design of longitudinal studies. *Cardiovasc Revasc Med.* 2024;58:79-87.

27. Jinnouchi H, Sato Y, Torii S, Sakamoto A, Cornelissen A, Bhoite RR, Kuntz S, Guo L, Paek KH, Fernandez R, Kolodgie FD, Virmani R, Finn AV. Detection of cholesterol crystals by optical coherence tomography. *EuroIntervention.* 2020;16:395-403.

28. Aoki T, Rodriguez-Porcel M, Matsuo Y, Cassar A, Kwon TG, Franchi F, Gulati R, Kushwaha SS, Lennon RJ, Lerman LO, Ritman EL, Lerman A. Evaluation of coronary adventitial vasa vasorum using 3D optical coherence tomography--animal and human studies. *Atherosclerosis.* 2015;239:203-8.

29. Kume T, Okura H, Yamada R, Koyama T, Fukuhara K, Kawamura A, Imai K, Neishi Y, Uemura S. Detection of Plaque Neovascularization by Optical Coherence Tomography: Ex Vivo Feasibility Study and In Vivo Observation in Patients With Angina Pectoris. *J Invasive Cardiol.* 2016;28:17-22.

30. Kubo T, Imanishi T, Takarada S, Kuroi A, Ueno S, Yamano T, Tanimoto T, Matsuo Y, Masho T, Kitabata H, Tsuda K, Tomobuchi Y, Akasaka T. Assessment of culprit lesion morphology in acute myocardial infarction: ability of optical coherence tomography compared with intravascular ultrasound and coronary angioscopy. *J Am Coll Cardiol.* 2007;50:933-9.

31. Groenland FTW, Ligthart JMR, Witberg KT, Daemen J. Patterns of intracoronary thrombus by high-definition intravascular ultrasound. *EuroIntervention.* 2022;18:e158-9.

32. Osinalde EP, Bastante T, Cecconi A, Muñiz ÁM, García-Guimaraes M, Rivero F, Rojas-González A, Olivera MJ, Salamanca J, de Isla LP, De Agustín JA, Caballero P, Torres RA, Jiménez-Borreguero LJ, Alfonso F. Intracoronary thrombus assessment with cardiac computed tomography angiography in a deferred stenting strategy: the MATURE prospective study (MSCT to Assess ThrombUs REsolution). *Coron Artery Dis.* 2023;34:167-76.

33. Achenbach S, Marwan M. Intracoronary thrombus. *J Cardiovasc Comput Tomogr.* 2009;3:344-5.

34. Jia H, Abtahian F, Aguirre AD, Lee S, Chia S, Lowe H, Kato K, Yonetsu T, Vergallo R, Hu S, Tian J, Lee H, Park SJ, Jang YS, Raffel OC, Mizuno K, Uemura S, Itoh T, Kakuta T, Choi SY, Dauerman HL, Prasad A, Toma C, McNulty I, Zhang S, Yu B, Fuster V, Narula J, Virmani R, Jang IK. In vivo diagnosis of plaque erosion and calcified nodule in patients with acute coronary syndrome by intravascular optical coherence tomography. *J Am Coll Cardiol.* 2013;62:1748-58.

35. Johnson TW, Räber L, di Mario C, Bourantas C, Jia H, Mattesini A, Gonzalo N, de la Torre Hernandez JM, Prati F, Koskinas K, Joner M, Radu MD, Erlinge D, Regar E, Kunadian V, Maehara A, Byrne RA, Capodanno D, Akasaka T, Wijns W, Mintz GS, Guagliumi G. Clinical use of intracoronary imaging. Part 2: acute coronary syndromes, ambiguous coronary angiography findings, and guiding interventional decision-making: an expert consensus document of the European Association of Percutaneous Cardiovascular Interventions. *Eur Heart J.* 2019;40:2566-84.

36. Matsumura M, Mintz GS, Kang SJ, Sum ST, Madden SP, Burke AP, Goldstein J, Parvataneni R, Stone GW, Muller JE, Virmani R, Maehara A. Intravascular ultrasound and near-infrared spectroscopic features of coronary lesions with intraplaque haemorrhage. *Eur Heart J Cardiovasc Imaging.* 2017;18:1222-8.

37. Cuesta J, Bastante T, Del Val D, Rivero F, Alfonso F. Plaque Progression Secondary to Intraplaque Hemorrhage Associated With Coronary Vasospasm. *JACC Cardiovasc Interv.* 2023;16:116-7.

38. Sano K, Kawasaki M, Ishihara Y, Okubo M, Tsuchiya K, Nishigaki K, Zhou X, Minatoguchi S, Fujita H, Fujiwara H. Assessment of vulnerable plaques causing acute coronary syndrome using integrated backscatter intravascular ultrasound. *J Am Coll Cardiol.* 2006;47:734-41.

39. Stone GW, Maehara A, Lansky AJ, de Bruyne B, Cristea E, Mintz GS, Mehran R, McPherson J, Farhat N, Marso SP, Parise H, Templin B, White R, Zhang Z, Serruys PW; PROSPECT Investigators. A prospective natural-history study of coronary atherosclerosis. *N Engl J Med.* 2011;364:226-35.

40. Calvert PA, Obaid DR, O'Sullivan M, Shapiro LM, McNab D, Densem CG, Schofield PM, Braganza D, Clarke SC, Ray KK, West NE, Bennett MR. Association between IVUS findings and adverse outcomes in patients with coronary artery disease: the VIVA (VH-IVUS in Vulnerable Atherosclerosis) Study. *JACC Cardiovasc Imaging.* 2011;4:894-901.

41. Cheng JM, Garcia-Garcia HM, de Boer SP, Kardys I, Heo JH, Akkerhuis KM, Oemrawsingh RM, van Domburg RT, Ligthart J, Witberg KT, Regar E, Serruys PW, van Geuns RJ, Boersma E. In vivo detection of high-risk coronary plaques by radiofrequency intravascular ultrasound and cardiovascular outcome: results of the ATHEROREMO-IVUS study. *Eur Heart J.* 2014;35:639-47.

42. Libby P, Pasterkamp G. Requiem for the 'vulnerable plaque'. *Eur Heart J.* 2015;36:2984-7.

43. Oemrawsingh RM, Cheng JM, García-García HM, van Geuns RJ, de Boer SP, Simsek C, Kardys I, Lenzen MJ, van Domburg RT, Regar E, Serruys PW, Akkerhuis KM, Boersma E; ATHEROREMO-NIRS Investigators. Near-infrared spectroscopy predicts cardiovascular outcome in patients with coronary artery disease. *J Am Coll Cardiol.* 2014;64:2510-8.

44. Erlinge D, Maehara A, Ben-Yehuda O, Bøtker HE, Maeng M, Kjøller-Hansen L, Engstrøm T, Matsumura M, Crowley A, Dressler O, Mintz GS, Fröbert O, Persson J, Wiseth R, Larsen AI, Okkels Jensen L, Nordrehaug JE, Bleie Ø, Omerovic E, Held C, James SK, Ali ZA, Muller JE, Stone GW; PROSPECT II Investigators. Identification of vulnerable plaques and patients by intracoronary near-infrared spectroscopy and ultrasound (PROSPECT II): a prospective natural history study. *Lancet.* 2021;397:985-95.

45. Prati F, Romagnoli E, Gatto L, La Manna A, Burzotta F, Ozaki Y, Marco V, Boi A, Fineschi M, Fabbiocchi F, Taglieri N, Niccoli G, Trani C, Versaci F, Calligaris G, Ruscica G, Di Giorgio A, Vergallo R, Albertucci M, Biondi-Zoccai G, Tamburino C, Crea F, Alfonso F, Arbustini E. Relationship between coronary plaque morphology of the left anterior descending artery and 12 months clinical outcome: the CLIMA study. *Eur Heart J.* 2020;41:383-91.

46. Kedhi E, Berta B, Roleder T, Hermanides RS, Fabris E, IJsselmuiden AJJ, Kauer F, Alfonso F, von Birgelen C, Escaned J, Camaro C, Kennedy MW, Pereira B, Magro M, Nef H, Reith S, Al Nooryani A, Rivero F, Malinowski K, De Luca G, Garcia Garcia H, Granada JF, Wojakowski W. Thin-cap fibroatheroma predicts clinical events in diabetic patients with normal fractional flow reserve: the COMBINE OCT-FFR trial. *Eur Heart J.* 2021;42:4671-9.

47. Jiang S, Fang C, Xu X, Xing L, Sun S, Peng C, Yin Y, Lei F, Wang Y, Li L, Chen Y, Pei X, Jia R, Tang C, Li S, Li S, Yu H, Chen T, Tan J, Liu X, Hou J, Dai J, Yu B. Identification of High-Risk Coronary Lesions by 3-Vessel Optical Coherence Tomography. *J Am Coll Cardiol.* 2023;81:1217-30.

48. Wykrzykowska JJ, Diletti R, Gutierrez-Chico JL, van Geuns RJ, van der Giessen WJ, Ramcharitar S, Duckers HE, Schultz C, de Feyter P, van der Ent M, Regar E, de Jaegere P, Garcia-Garcia HM, Pawar R, Gonzalo N, Ligthart J, de Schepper J, van den Berg N, Milewski K, Granada JF, Serruys PW. Plaque sealing and passivation with a mechanical self-expanding low outward force nitinol vShield device for the treatment of IVUS and OCT-derived thin cap fibroatheromas (TCFAs) in native coronary arteries:

report of the pilot study vShield Evaluated at Cardiac hospital in Rotterdam for Investigation and Treatment of TCFA (SECRITT). *EuroIntervention*. 2012;8:945-54.

49. Stone GW, Maehara A, Ali ZA, Held C, Matsumura M, Kjøller-Hansen L, Bøtker HE, Maeng M, Engstrøm T, Wiseth R, Persson J, Trovik T, Jensen U, James SK, Mintz GS, Dressler O, Crowley A, Ben-Yehuda O, Erlinge D; PROSPECT ABSORB Investigators. Percutaneous Coronary Intervention for Vulnerable Coronary Atherosclerotic Plaque. *J Am Coll Cardiol*. 2020;76:2289-301.

50. Hong MK, Mintz GS, Lee CW, Kim YH, Lee SW, Song JM, Han KH, Kang DH, Song JK, Kim JJ, Park SW, Park SJ. Comparison of coronary plaque rupture between stable angina and acute myocardial infarction: a three-vessel intravascular ultrasound study in 235 patients. *Circulation*. 2004;110:928-33.

51. Maehara A, Mintz GS, Bui AB, Walter OR, Castagna MT, Canos D, Pichard AD, Satler LF, Waksman R, Suddath WO, Laird JR Jr, Kent KM, Weissman NJ. Morphologic and angiographic features of coronary plaque rupture detected by intravascular ultrasound. *J Am Coll Cardiol*. 2002;40:904-10.

52. Scheller B, Ohlow MA, Ewen S, Kische S, Rudolph TK, Clever YP, Wagner A, Richter S, El-Garhy M, Böhm M, Degenhardt R, Mahfoud F, Lauer B. Bare metal or drug-eluting stent versus drug-coated balloon in non-ST-elevation myocardial infarction: the randomised PEPCAD NSTEMI trial. *EuroIntervention*. 2020;15:1527-33.

53. Ho HH, Tan J, Ooi YW, Loh KK, Aung TH, Yin NT, Sinaga DA, Jafary FH, Ong PJ. Preliminary experience with drug-coated balloon angioplasty in primary percutaneous coronary intervention. *World J Cardiol*. 2015;7:311-4.

54. Vos NS, Dirksen MT, Vink MA, van Nooijen FC, Amoroso G, Herrman JP, Kiemeneij F, Patterson MS, Slagboom T, van der Schaaf RJ. Safety and feasibility of a PAclitaxel-eluting balloon angioplasty in Primary Percutaneous coronary intervention in Amsterdam (PAPPA): one-year clinical outcome of a pilot study. *EuroIntervention*. 2014;10:584-90.

55. Gobić D, Tomulić V, Lulić D, Židan D, Brusich S, Jakljević T, Zaputović L. Drug-Coated Balloon Versus Drug-Eluting Stent in Primary Percutaneous Coronary Intervention: A Feasibility Study. *Am J Med Sci*. 2017;354:553-60.

56. Belkacemi A, Agostoni P, Nathoe HM, Voskuil M, Shao C, Van Belle E, Wildbergh T, Politi L, Doevendans PA, Sangiorgi GM, Stella PR. First results of the DEB-AMI (drug eluting balloon in acute ST-segment elevation myocardial infarction) trial: a multicenter randomized comparison of drug-eluting balloon plus bare-metal stent versus bare-metal stent versus drug-eluting stent in primary percutaneous coronary intervention with 6-month angiographic, intravascular, functional, and clinical outcomes. *J Am Coll Cardiol*. 2012;59:2327-37.

57. Vos NS, Fagel ND, Amoroso G, Herrman JR, Patterson MS, Piers LH, van der Schaaf RJ, Slagboom T, Vink MA. Paclitaxel-Coated Balloon Angioplasty Versus Drug-Eluting Stent in Acute Myocardial Infarction: The REVELATION Randomized Trial. *JACC Cardiovasc Interv*. 2019;12:1691-9.

58. Niccoli G, Montone RA, Di Vito L, Gramegna M, Refaat H, Scalone G, Leone AM, Trani C, Burzotta F, Porto I, Aurigemma C, Prati F, Crea F. Plaque rupture and intact fibrous cap assessed by optical coherence tomography portend different outcomes in patients with acute coronary syndrome. *Eur Heart J*. 2015;36:1377-84.

59. Higuma T, Soeda T, Abe N, Yamada M, Yokoyama H, Shibutani S, Vergallo R, Minami Y, Ong DS, Lee H, Okumura K, Jang IK. A Combined Optical Coherence Tomography and Intravascular Ultrasound Study on Plaque Rupture, Plaque Erosion, and Calcified Nodule in Patients With ST-Segment Elevation Myocardial Infarction: Incidence, Morphologic Characteristics, and Outcomes After Percutaneous Coronary Intervention. *JACC Cardiovasc Interv*. 2015;8:1166-76.

60. Prati F, Uemura S, Souteyrand G, Virmani R, Motreff P, Di Vito L, Biondi-Zoccai G, Halperin J, Fuster V, Ozaki Y, Narula J. OCT-based diagnosis and management of STEMI associated with intact fibrous cap. *JACC Cardiovasc Imaging*. 2013;6:283-7.

61. Jia H, Dai J, Hou J, Xing L, Ma L, Liu H, Xu M, Yao Y, Hu S, Yamamoto E, Lee H, Zhang S, Yu B, Jang IK. Effective anti-thrombotic therapy without stenting: intravascular optical coherence tomography-based management in plaque erosion (the EROSION study). *Eur Heart J*. 2017;38:792-800.

62. Xing L, Yamamoto E, Sugiyama T, Jia H, Ma L, Hu S, Wang C, Zhu Y, Li L, Xu M, Liu H, Bryniarski K, Hou J, Zhang S, Lee H, Yu B, Jang IK. EROSION Study (Effective Anti-Thrombotic Therapy Without Stenting: Intravascular Optical Coherence Tomography-Based Management in Plaque Erosion): A 1-Year Follow-Up Report. *Circ Cardiovasc Interv*. 2017;10:e005860.

63. Jia H, Dai J, He L, Xu Y, Shi Y, Zhao L, Sun Z, Liu Y, Weng Z, Feng X, Zhang D, Chen T, Zhang X, Li L, Xu Y, Wu Y, Yang Y, Wang C, Li L, Li J, Hou J, Liu B, Mintz GS, Yu B. EROSION III: A Multicenter RCT of OCT-Guided Reperfusion in STEMI With Early Infarct Artery Patency. *JACC Cardiovasc Interv*. 2022;15:846-56.

64. Torii S, Jinnouchi H, Sakamoto A, Mori H, Park J, Amoa FC, Sawan M, Sato Y, Cornelissen A, Kuntz SH, Kutyna M, Paek KH, Fernandez R, Braumann R, Mont EK, Surve D, Romero ME, Kolodgie FD, Virmani R, Finn AV. Vascular responses to coronary calcification following implantation of newer-generation drug-eluting stents in humans: impact on healing. *Eur Heart J*. 2020;41:786-96.

65. Bourantas CV, Zhang YJ, Garg S, Iqbal J, Valgimigli M, Windecker S, Mohr FW, Silber S, Vries Td, Onuma Y, Garcia-Garcia HM, Morel MA, Serruys PW. Prognostic implications of coronary calcification in patients with obstructive coronary artery disease treated by percutaneous coronary intervention: a patient-level pooled analysis of 7 contemporary stent trials. *Heart*. 2014;100:1158-64.

66. Généreux P, Madhavan MV, Mintz GS, Maehara A, Palmerini T, Lasalle L, Xu K, McAndrew T, Kirtane A, Lansky AJ, Brener SJ, Mehran R, Stone GW. Ischemic outcomes after coronary intervention of calcified vessels in acute coronary syndromes. Pooled analysis from the HORIZONS-AMI (Harmonizing Outcomes With Revascularization and Stents in Acute Myocardial Infarction) and ACUITY (Acute Catheterization and Urgent Intervention Triage Strategy) TRIALS. *J Am Coll Cardiol*. 2014;63:1845-54.

67. Alfonso F, Gonzalo N, Nuñez-Gil I, Bañuelos C. Coronary thrombosis from large, nonprotruding, superficial calcified coronary plaques. *J Am Coll Cardiol*. 2013;62:2254.

68. Sugiyama T, Yamamoto E, Fracassi F, Lee H, Yonetsu T, Kakuta T, Soeda T, Saito Y, Yan BP, Kurihara O, Takano M, Niccoli G, Crea F, Higuma T, Kimura S, Minami Y, Ako J, Adriaenssens T, Boeder NF, Nef HM, Fujimoto JG, Fuster V, Finn AV, Falk E, Jang IK. Calcified Plaques in Patients With Acute Coronary Syndromes. *JACC Cardiovasc Interv*. 2019;12:531-40.

69. Garcia-Garcia HM, Costa MA, Serruys PW. Imaging of coronary atherosclerosis: intravascular ultrasound. *Eur Heart J*. 2010;31:2456-69.

70. Räber L, Ueki Y, Otsuka T, Losdat S, Häner JD, Lonborg J, Fahrni G, Iglesias JF, van Geuns RJ, Ondracek AS, Radu Juul Jensen MD, Zanchin C, Stortecky S, Spirk D, Siontis GCM, Saleh L, Matter CM, Daemen J, Mach F, Heg D, Windecker S, Engstrøm T, Lang IM, Koskinas KC; PACMAN-AMI collaborators. Effect of Alirocumab Added to High-Intensity Statin Therapy on Coronary Atherosclerosis in Patients With Acute Myocardial Infarction: The PACMAN-AMI Randomized Clinical Trial. *JAMA*. 2022;327:1771-81.

71. Nissen SE, Tuzcu EM, Schoenhagen P, Brown BG, Ganz P, Vogel RA, Crowe T, Howard G, Cooper CJ, Brodie B, Grines CL, DeMaria AN; REVERSAL Investigators. Effect of intensive compared with moderate lipid-lowering therapy on progression of coronary atherosclerosis: a randomized controlled trial. *JAMA*. 2004;291:1071-80.

72. Nissen SE, Nicholls SJ, Sipahi I, Libby P, Raichlen JS, Ballantyne CM, Davignon J, Erbel R, Fruchart JC, apo JC, Schoenhagen P, Crowe T, Cain V, Wolski K, Goormastic M, Tuzcu EM; ASTEROID Investigators. Effect of very high-intensity statin therapy on regression of coronary atherosclerosis: the ASTEROID trial. *JAMA*. 2006;295:1556-65.

73. Nicholls SJ, Ballantyne CM, Barter PJ, Chapman MJ, Erbel RM, Libby P, Raichlen JS, Uno K, Borgman M, Wolski K, Nissen SE. Effect of two intensive statin regimens on progression of coronary disease. *N Engl J Med*. 2011;365:2078-87.

74. Hibi K, Sonoda S, Kawasaki M, Otsuji Y, Murohara T, Ishii H, Sato K, Koshida R, Ozaki Y, Sata M, Morino Y, Miyamoto T, Amano T, Morita S,

Kozuma K, Kimura K, Fujiwara H; Ezetimibe-ACS Investigators. Effects of Ezetimibe-Statin Combination Therapy on Coronary Atherosclerosis in Acute Coronary Syndrome. *Circ J*. 2018;82:757-66.

75. Kovarnik T, Mintz GS, Skalicka H, Kral A, Horak J, Skulec R, Uhrova J, Martasek P, Downe RW, Wahle A, Sonka M, Mrazek V, Aschermann M, Linhart A. Virtual histology evaluation of atherosclerosis regression during atorvastatin and ezetimibe administration: HEAVEN study. *Circ J*. 2012;76:176-83.

76. Nakajima N, Miyauchi K, Yokoyama T, Ogita M, Miyazaki T, Tamura H, Nishino A, Yokoyama K, Okazaki S, Kurata T, Suwa S, Daida H. Effect of combination of ezetimibe and a statin on coronary plaque regression in patients with acute coronary syndrome: ZEUS trial (eZEtimibe Ultrasound Study). *IJC Metabolic & Endocrine*. 2014;3:8-13.

77. Tsujita K, Sugiyama S, Sumida H, Shimomura H, Yamashita T, Yamanaga K, Komura N, Sakamoto K, Oka H, Nakao K, Nakamura S, Ishihara M, Matsui K, Sakaino N, Nakamura N, Yamamoto N, Koide S, Matsumura T, Fujimoto K, Tsunoda R, Morikami Y, Matsuyama K, Oshima S, Kaikita K, Hokimoto S, Ogawa H; PRECISE–IVUS Investigators. Impact of Dual Lipid-Lowering Strategy With Ezetimibe and Atorvastatin on Coronary Plaque Regression in Patients With Percutaneous Coronary Intervention: The Multicenter Randomized Controlled PRECISE-IVUS Trial. *J Am Coll Cardiol*. 2015;66:495-507.

78. Nicholls SJ, Puri R, Anderson T, Ballantyne CM, Cho L, Kastelein JJ, Koenig W, Somaratne R, Kassahun H, Yang J, Wasserman SM, Scott R, Ungi I, Podolec J, Ophuis AO, Cornel JH, Borgman M, Brennan DM, Nissen SE. Effect of Evolocumab on Progression of Coronary Disease in Statin-Treated Patients: The GLAGOV Randomized Clinical Trial. *JAMA*. 2016;316:2373-84.

79. Nicholls SJ, Kataoka Y, Nissen SE, Prati F, Windecker S, Puri R, Hucko T, Aradi D, Herrman JR, Hermanides RS, Wang B, Wang H, Butters J, Di Giovanni G, Jones S, Pompili G, Psaltis PJ. Effect of Evolocumab on Coronary Plaque Phenotype and Burden in Statin-Treated Patients Following Myocardial Infarction. *JACC Cardiovasc Imaging*. 2022;15:1308-21.

80. Ako J, Hibi K, Tsujita K, Hiro T, Morino Y, Kozuma K, Shinke T, Otake H, Uno K, Louie MJ, Takagi Y, Miyauchi K. Effect of Alirocumab on Coronary Atheroma Volume in Japanese Patients With Acute Coronary Syndrome - The ODYSSEY J-IVUS Trial. *Circ J*. 2019;83:2025-33.

81. Soma MR, Donetti E, Parolini C, Sirtori CR, Fumagalli R, Franceschini G. Recombinant apolipoprotein A-IMilano dimer inhibits carotid intimal thickening induced by perivascular manipulation in rabbits. *Circ Res*. 1995;76:405-11.

82. Nissen SE, Tsunoda T, Tuzcu EM, Schoenhagen P, Cooper CJ, Yasin M, Eaton GM, Lauer MA, Sheldon WS, Grines CL, Halpern S, Crowe T, Blankenship JC, Kerensky R. Effect of recombinant ApoA-I Milano on coronary atherosclerosis in patients with acute coronary syndromes: a randomized controlled trial. *JAMA*. 2003;290:2292-300.

83. Gibson CM, Duffy D, Korjian S, Bahit MC, Chi G, Alexander JH, Lincoff AM, Heise M, Tricoci P, Deckelbaum LI, Mears SJ, Nicolau JC, Lopes RD, Merkely B, Lewis BS, Cornel JH, Trebacz J, Parkhomenko A, Libby P, Sacks FM, Povsic TJ, Bonaca M, Goodman SG, Bhatt DL, Tendera M, Steg PG, Ridker PM, Aylward P, Kastelein JJP, Bode C, Mahaffey KW, Nicholls SJ, Pocock SJ, Mehran R, Harrington RA; AEGIS-II Committees and Investigators. Apolipoprotein A1 Infusions and Cardiovascular Outcomes after Acute Myocardial Infarction. *N Engl J Med*. 2024;390:1560-71.

84. Nissen SE, Nicholls SJ, Wolski K, Nesto R, Kupfer S, Perez A, Jure H, De Larochellière R, Staniloae CS, Mavromatis K, Saw J, Hu B, Lincoff AM, Tuzcu EM; PERISCOPE Investigators. Comparison of pioglitazone vs glimepiride on progression of coronary atherosclerosis in patients with type 2 diabetes: the PERISCOPE randomized controlled trial. *JAMA*. 2008;299:1561-73.

85. Gerstein HC, Ratner RE, Cannon CP, Serruys PW, García-García HM, van Es GA, Kolatkar NS, Kravitz BG, Miller DM, Huang C, Fitzgerald PJ, Nesto RW; APPROACH Study Group. Effect of rosiglitazone on progression of coronary atherosclerosis in patients with type 2 diabetes mellitus and coronary artery disease: the assessment on the prevention of progression by rosiglitazone on atherosclerosis in diabetes patients with cardiovascular history trial. *Circulation*. 2010;121:1176-87.

86. Nissen SE, Tuzcu EM, Libby P, Thompson PD, Ghali M, Garza D, Berman L, Shi H, Buebendorf E, Topol EJ; CAMELOT Investigators. Effect of antihypertensive agents on cardiovascular events in patients with coronary disease and normal blood pressure: the CAMELOT study: a randomized controlled trial. *JAMA*. 2004;292:2217-25.

87. Rodriguez-Granillo GA, Vos J, Bruining N, Garcia-Garcia HM, de Winter S, Ligthart JM, Deckers JW, Bertrand M, Simoons ML, Ferrari R, Fox KM, Remme W, De Feyter PJ; Investigators of the EUROPA Study. Long-term effect of perindopril on coronary atherosclerosis progression (from the perindopril's prospective effect on coronary atherosclerosis by angiography and intravascular ultrasound evaluation [PERSPECTIVE] study). *Am J Cardiol*. 2007;100:159-63.

88. Hirohata A, Yamamoto K, Miyoshi T, Hatanaka K, Hirohata S, Yamawaki H, Komatsubara I, Murakami M, Hirose E, Sato S, Ohkawa K, Ishizawa M, Yamaji H, Kawamura H, Kusachi S, Murakami T, Hina K, Ohe T. Impact of olmesartan on progression of coronary atherosclerosis a serial volumetric intravascular ultrasound analysis from the OLIVUS (impact of OLmesarten on progression of coronary atherosclerosis: evaluation by intravascular ultrasound) trial. *J Am Coll Cardiol*. 2010;55:976-82.

89. Nicholls SJ, Bakris GL, Kastelein JJ, Menon V, Williams B, Armbrecht J, Brunel P, Nicolaides M, Hsu A, Hu B, Fang H, Puri R, Uno K, Kataoka Y, Bash D, Nissen SE. Effect of aliskiren on progression of coronary disease in patients with prehypertension: the AQUARIUS randomized clinical trial. *JAMA*. 2013;310:1135-44.

90. Ozaki Y, Garcia-Garcia HM, Beyene SS, Hideo-Kajita A, Kuku KO, Kolm P, Waksman R. Effect of Statin Therapy on Fibrous Cap Thickness in Coronary Plaque on Optical Coherence Tomography - Review and Meta-Analysis. *Circ J*. 2019;83:1480-8.

91. Räber L, Koskinas KC, Yamaji K, Taniwaki M, Roffi M, Holmvang L, Garcia Garcia HM, Zanchin T, Maldonado R, Moschovitis A, Pedrazzini G, Zaugg S, Dijkstra J, Matter CM, Serruys PW, Lüscher TF, Kelbaek H, Karagiannis A, Radu MD, Windecker S. Changes in Coronary Plaque Composition in Patients With Acute Myocardial Infarction Treated With High-Intensity Statin Therapy (IBIS-4): A Serial Optical Coherence Tomography Study. *JACC Cardiovasc Imaging*. 2019;12:1518-28.

92. Sugizaki Y, Otake H, Kawamori H, Toba T, Nagano Y, Tsukiyama Y, Yanaka KI, Yamamoto H, Nagasawa A, Onishi H, Takeshige R, Nakano S, Matsuoka Y, Tanimura K, Takahashi Y, Fukuyama Y, Shinke T, Ishida T, Hirata KI. Adding Alirocumab to Rosuvastatin Helps Reduce the Vulnerability of Thin-Cap Fibroatheroma: An ALTAIR Trial Report. *JACC Cardiovasc Imaging*. 2020;13:1452-4.

93. Räber L, Taniwaki M, Zaugg S, Kelbæk H, Roffi M, Holmvang L, Noble S, Pedrazzini G, Moschovitis A, Lüscher TF, Matter CM, Serruys PW, Jüni P, Garcia-Garcia HM, Windecker S; IBIS 4 (Integrated Biomarkers and Imaging Study-4) Trial Investigators (NCT00962416). Effect of high-intensity statin therapy on atherosclerosis in non-infarct-related coronary arteries (IBIS-4): a serial intravascular ultrasonography study. *Eur Heart J*. 2015;36:490-500.

94. Daida H, Takayama T, Hiro T, Yamagishi M, Hirayama A, Saito S, Yamaguchi T, Matsuzaki M; COSMOS Investigators. High HbA1c levels correlate with reduced plaque regression during statin treatment in patients with stable coronary artery disease: results of the coronary atherosclerosis study measuring effects of rosuvastatin using intravascular ultrasound in Japanese subjects (COSMOS). *Cardiovasc Diabetol*. 2012;11:87.

95. Park SJ, Kang SJ, Ahn JM, Chang M, Yun SC, Roh JH, Lee PH, Park HW, Yoon SH, Park DW, Lee SW, Kim YH, Lee CW, Mintz GS, Han KH, Park SW. Effect of Statin Treatment on Modifying Plaque Composition: A Double-Blind, Randomized Study. *J Am Coll Cardiol*. 2016;67:1772-83.

96. Hiro T, Kimura T, Morimoto T, Miyauchi K, Nakagawa Y, Yamagishi M, Ozaki Y, Kimura K, Saito S, Yamaguchi T, Daida H, Matsuzaki M; JAPAN-ACS Investigators. Effect of intensive statin therapy on regression of coronary atherosclerosis in patients with acute coronary syndrome: a multicenter randomized trial evaluated by volumetric intravascular ultrasound using pitavastatin versus atorvastatin (JAPAN-ACS [Japan assessment of pitavastatin and atorvastatin in acute coronary syndrome] study). *J Am Coll Cardiol*. 2009;54:293-302.

97. Nissen SE, Tardif JC, Nicholls SJ, Revkin JH, Shear CL, Duggan WT, Ruzyllo W, Bachinsky WB, Lasala GP, Tuzcu EM; ILLUSTRATE Investigators. Effect of torcetrapib on the progression of coronary atherosclerosis. *N Engl J Med*. 2007;356:1304-16.

98. Watanabe T, Ando K, Daidoji H, Otaki Y, Sugawara S, Matsui M, Ikeno E, Hirono O, Miyawaki H, Yashiro Y, Nishiyama S, Arimoto T, Takahashi H, Shishido T, Miyashita T, Miyamoto T, Kubota I; CHERRY study investigators. A randomized controlled trial of eicosapentaenoic acid in patients with coronary heart disease on statins. *J Cardiol*. 2017;70:537-44.

99. Tardif JC, Ballantyne CM, Barter P, Dasseux JL, Fayad ZA, Guertin MC, Kastelein JJ, Keyserling C, Klepp H, Koenig W, L'Allier PL, Lespérance J, Lüscher TF, Paolini JF, Tawakol A, Waters DD; Can HDL Infusions Significantly QUicken Atherosclerosis REgression (CHI-SQUARE) Investigators. Effects of the high-density lipoprotein mimetic agent CER-001 on coronary atherosclerosis in patients with acute coronary syndromes: a randomized trial. *Eur Heart J*. 2014;35:3277-86.

100. Nicholls SJ, Andrews J, Kastelein JJP, Merkely B, Nissen SE, Ray KK, Schwartz GG, Worthley SG, Keyserling C, Dasseux JL, Griffith L, Kim SW, Janssan A, Di Giovanni G, Pisaniello AD, Scherer DJ, Psaltis PJ, Butters J. Effect of Serial Infusions of CER-001, a Pre-β High-Density Lipoprotein Mimetic, on Coronary Atherosclerosis in Patients Following Acute Coronary Syndromes in the CER-001 Atherosclerosis Regression Acute Coronary Syndrome Trial: A Randomized Clinical Trial. *JAMA Cardiol*. 2018;3:815-22.

101. Otsuka F, Joner M, Prati F, Virmani R, Narula J. Clinical classification of plaque morphology in coronary disease. *Nat Rev Cardiol*. 2014;11:379-89.

Supplementary data

Supplementary Appendix 1. A natural history of atherosclerosis.

Supplementary Table 1. Tissue types: preferred descriptive names.

Supplementary Figure 1. Machine learning machinery applied to imaging of atherosclerosis.

Moving image 1. Lipid- and necrotic core-rich plaques.

Moving image 2. Calcified plaques.

Moving image 3. Thrombotic plaques.

Moving image 4. Plaque types: revised nomenclature.

Moving image 5. Main high-risk plaque characteristics.

The supplementary data are published online at: https://eurointervention.pcronline.com/doi/10.4244/EIJ-D-24-00387

Supplementary data

Supplementary Appendix 1. A natural history of atherosclerosis.

What is atherosclerosis and its clinical manifestations?

Atherosclerosis is a disease that takes place within the intima layer of the vasculature; plaque formation is initiated by migration of monocytes and lymphocytes with subsequent lipid uptake and foam cells formation; in addition, there is smooth muscle cell migration and proliferation of extracellular matrix leading to the formation of *adaptative intimal thickening* (AIT). The interplay between lipid accumulation and inflammation are the two most pathognomonic characteristics of the near life-long lasting process since it is thought to commence at the very early stages of the human and other primates' species life. The AITs may affect the entire vasculature but tend to accumulate in areas of distributed blood flow such as in curved vessels and in branching points particularly the outer walls of bifurcation and progress in an independent manner through the continuous lipid accumulation and inflammatory process with some of them evolving into *pathological intimal thickening* (PIT)[1]. Calcifications may be present in PIT as microcalcifications (<0.5 to 15 μm)[2]. The *lipid pool* is acellular and contains abundant proteoglycans and lipid. When macrophages incorporate the lipid from the pool, they experience apoptosis and form acellular debris that all together form the *necrotic core*. (3) The free cholesterol, which also comes from red cells, crystalizes and form the so-called *cholesterol crystals (CCR)*[3]. In turn, CCR trigger inflammation which perpetuates necrotic core formation.

Fibroatheroma is the pathological landmark of atherosclerosis. In its early stages is mainly composed by lipid, necrotic core, inflammatory cells, cellular debris and calcifications and is covered by a fibrous cap which may become thinner and weakened over time leading to the formation of the *thin-capped fibroatheroma* (TCFA – the so called "vulnerable plaque"). TCFA is the most common cause of plaque rupture and its consequent coronary thrombosis, accounting for 2/3 of the acute coronary syndromes[4]. **Figure 1 of the main text.** The remaining ACS events are caused either by plaque erosion (PE) or by eruption of a calcified nodules (CN).

Plaque erosion is defined as a loss of the endothelial lining with lacerations of the superficial intimal layers in the absence of "trans-cap" ruptures. Plaque erosion occur over lesions rich in smooth muscle cells and proteoglycans that may hold extracellular lipid pools in the deep intima, but superficial necrotic cores are uncommon[5].

Calcified nodule is an eruptive (often called *eruptive calcified nodule*) calcified mass showing an irregular disrupted surface which tends to be associated with heavily calcified plaques, and some include bony spicules and interspersed fibrin; It is suggested that platelet deposition subsequently accrues on top of a fibrin-rich thrombus[5]. Therefore, the term eruptive CN is reserved for lesions resulting in plaque complication leading to arterial thrombosis.

Nodular calcification, alternatively, is a term reserved for innocent non-culprit or by-standard lesions, which also have a convex like calcium shape with preserved endothelial coverage (*non-eruptive calcified nodule*), that are not associated with intraluminal thrombosis[6].

Fibrocalcific lesions are those with dense calcium. They consist of deposits of hydroxyapatite (crystallization of calcium/phosphate) in the extracellular matrix of the arterial wall. There are two types of vascular calcification: 1) atherosclerotic intimal calcification and 2) medial calcification, also called Monckeberg's calcification[2].

Intraplaque hemorrhage has been found in association with large necrotic cores and advanced stages of atherosclerosis, particularly in those plaques with signs of instability[7]. It may be explained by the accumulation of free cholesterol released from the erythrocyte membranes. The erythrocyte contains a specific protein, glycophorin A. The degree of glycophorin A reactivity and the iron deposition correlated positively with the size of necrotic core and the density of macrophage infiltration.

A breech in the medial wall has been suggested to facilitate the rapid in-growth of *microvessels* from the adventitia, and exposure to an atherosclerotic environment stimulates abnormal vascular development characterized by disorganized branching and immature endothelial tubes with "leaky" imperfect linings. This network of immature blood vessels might also be a source of intraplaque hemorrhage providing erythrocyte-derived phospholipids and free cholesterol. By contributing to the deposition of free cholesterol, macrophage infiltration, and enlargement of the necrotic core, the accumulation of erythrocyte membranes within an atherosclerotic plaque represents a potent atherogenic stimulus. All these factors appear to increase the risk of plaque progression and destabilization. Although intraplaque hemorrhage has been reported to be common in pathological studies of patients with advanced coronary atherosclerotic lesions the diagnosis of this anatomic entity in the clinical setting has been until now largely elusive.

Healed plaques. Mann and Davies[8] suggested the role of "*subclinical*" episodes of plaque disruption and healing as a mechanism of phasic coronary plaque growth in men who died suddenly. A subsequent pathological study confirmed that 75% of ruptured plaques had evidence of previous ruptures[9]. The lumen narrowing increased linearly with the number of visualized healed ruptures. The hallmark of plaque healing is the presence of distinct layers of fibrotic tissue (first loosely arranged collagen type III and thereafter dense type I) overlying plaques with previous rupture or erosion[10]. Intraluminal thrombus may become organized and progressively incorporated into the vessel causing plaque progression[9,10]. Infiltration of inflammatory and smooth-muscle cells, neoangiogenesis and deposition of extracellular matrix and proteoglycans play a major role in the process of thrombus organization.

Neoatherosclerosis is a process that develops within metallic stents and is characterized by the presence of lipid-laden macrophages within the neointima. Later stages of neoatherosclerosis may show necrotic cores/calcifications.

Following the implantation of the stents, neointimal healing starts to form. Although newer generation drug eluting stents (DES) are antithrombogenic, the early phase is characterized by thrombus/fibrin deposition either as protruding thrombi from the native ruptured plaque or due to the binding of some degree of fibrinogen[11]. An intravascular imaging study showed co-localization of the acutely seen thrombotic deposit and the layers of neointima in the follow-up[12]. Coverage of the struts with "new" tissue prevents stent thrombosis[11].

Chronic stable coronary syndrome is the most prevalent form of coronary atherosclerosis which tends to appear late in the natural history of atherosclerosis and its most common clinical presentation is exertional angina symptoms attributed to myocardial ischemia because of lumen narrowing. Lumen obstruction appears in lesions with increased plaque burden as in the early stages of atherosclerosis the outer vessel wall can expand and accommodate the plaque growth. Only when the plaque burden exceeds the cutoff of 40% the plaque starts affecting the patency of the lumen as the vessel wall cannot longer expand. This process was first documented by Glagov et al. and is also known as *positive remodeling*[13].

Thus, the occurrence of flow limiting stenosis may occur progressively, as the result of silent plaque accumulation and failure of the vessel to remodel and preserve the lumen, sub-acutely, as the result of rapid plaque progression occurred during the healing process

of destabilized plaques or acutely because of vessel occlusion induced by PR, PE or an erupted CN leading to an *acute myocardial infarction* (MI). **Figure 3 of the main text.**

Fundamentals of intravascular imaging

Unlike coronary angiography that only outlines the coronary lumen and its contents (i.e. thrombus) and is unable to assess the vessel wall's composition where the coronary atherosclerosis is present, intravascular imaging does visualize directly the vessel wall and lumen contents.

Coronary computed tomography angiography (CCTA) in a non-invasive, full coronary tree imaging modality that can provide information about the accumulation of plaque in the vessel wall and whether the plaque has affected the luminal dimensions. CCTA can also give information about plaque composition as Hounsfield units values differ in calcific, fibrotic and lipid-rich lesions and also enables detection of distinct plaque layouts such as "napkin-ring" sign and spotty calcification[14,15]. **Figure 2, Table 1 both main text.**

Intravascular ultrasound (IVUS), which is an invasive imaging modality, has better resolution (~150 μm), and allows more accurate quantification of the plaque burden and the lumen dimensions than CCTA. It does also provide valuable insights into different plaque tissues such as fibrous, calcium and lipid. **Table 2 main text.**

Optical coherence tomography (OCT), with the best axial resolution (~15 μm) from all coronary imaging modalities, is also an invasive diagnostic tool that enables accurate quantification of lumen and plaque areas. Its main contribution is unraveling unique information on the distinct morphological features of the culprit lesions such as plaque rupture (PR), plaque erosion and calcified nodules and their associated thrombosis[16]. **Figure 3 main text**. The 2023 ESC Guidelines for the management of acute coronary syndromes recommend to use OCT in patients with ambiguous culprit lesion (Class IIb) and in cases of myocardial infarction with non-obstructive coronary arteries (MINOCA)[17].

How to assess atherosclerotic plaque size and its components

Plaque (also known as atheroma) is the generic term to refer to the contents between the *lumen area* (drawn at the interface between the space where the blood flows and vessel wall) and the most outer (trailing edge) of the media which coincides with the location of the external elastic membrane (EEM, or lamina, EEL). The EEM was chosen, as opposed to the internal EM (IEM) because the IEM is often not discernable with IVUS/CCTA imaging. In this document, we will use the term "*vessel" area* to refer to the EEM area. **Figure 4 main text.**

Earlier we mentioned that atherosclerosis is a disease of the intima layer, but all imaging modalities include the media in the measurements and therefore technically the plaque always includes the media layer. For reporting purposes, we propose to simply use the term plaque area and an intimal thickness $\geq$0.5 mm to be defined as atherosclerotic[18]. Most atherosclerotic plaques portrait three predominant tissue types: lipid, calcium and fibrous (most abundant) which all together explain most of the atherosclerotic plaque contents. In the next sections, we describe each of them individually.

Plaque burden is the preferred term to describe the relative amount of plaque area that is contained within the vessel area. Thus, plaque burden is plaque area divided by vessel area and is presented as a percentage. **Figure 4 main text.**

Progression/regression coronary imaging trials have used the derived volumetric equivalents to plaque area which is total atheroma volume (TAV) and percentage atheroma volume (PAV). To assess progression regression the EEM should be clearly visualized and in this regard the lower penetration of OCT as compared with IVUS should be considered[19].

Artificial intelligence in imaging of atherosclerosis

Generally speaking, the assessment of atherosclerotic disease in all its forms requires intensive qualitative and quantitative analysis, which is highly endangered with intra- and inter-observer variability. Thus, reproducibility and reliability of the results remain the weak links in the characterization and analysis of atherosclerotic disease. In this regard, the whole drift of algorithmic solutions towards artificial intelligence-based tools emerges as a promising area of research with vital implications in the field.

Artificial intelligence (AI) emerged in the 50s as a strategy to emulate the human capabilities at problem-solving, in situations where handcrafting rules is a difficult task. This approach leverages the information contained in large datasets, sometimes supervised by human expertise, to deliver expert systems capable of performing classification/regression procedures. Machine learning (ML) as a subfield of AI has been systematically employed in computer vision due to the advent of specific hardware (graphic processing units), and software infrastructure to exploit such hardware. These ML algorithms gained the community's attention because of the flexibility in producing complex tasks based on the rules learned during the so-called learning stage. However, ML models still require considerable human intervention to learn. Within ML models, deep learning (DL) models stand out as a more powerful approach to solve more complex tasks, such as semantic image segmentation [10.1109/CVPR.2015.7298965], where DL models have dominated the landscape in the last years showing state-of-the-art performance with minimal human intervention. The development of supervised ML and DL models requires large amounts of data to find the optimal parameters that define the model (training/validation phases), and demands for proper insight into the most convenient metrics to assess the performance of the model during operation (testing phase). Datasets have to be adequately curated so, when the model is exposed to new data, they can perform consistently with the results delivered during training/validation phases. In this sense, the model must be trained on the same type of data than the data the model will be exposed during operation. A badly trained AI algorithm is like a badly trained physician, it will definitely deliver bad outcomes. When properly trained, many tasks involving the characterization of atherosclerotic disease can be tackled using ML and DL models, and there is plenty room for research and applications where such kind of models can outperform current technologies.

AI, and specifically research in ML/DL models, has exploded in the last years among the different image modalities of relevance in the assessment of atherosclerotic plaques

(IVUS, OCT and CCTA), showing promising results. The increasing availability of imaging protocols yielded a substantial amount of data to be analyzed, and the possibility of inquiring into details that had been previously overlooked. Image-based analysis of atherosclerosis implies extracting quantitative measures and features from medical images to define the plaque composition and risk it poses to the patient, the size and the extension of the plaque within the vascular wall at a certain time, and more importantly the evolution (progression/regression) experimented along time, enabling a holistic risk assessment.

Determination of coronary stenoses, and quantification of plaque atheroma volume and composition, as well as extraction of length and angle of calcified regions by AI algorithms will help to overcome these time-consuming and expertise-demanding tasks[20]. The same applies to radiomics, which proved robust in identifying certain types of plaques, and for which automated analysis through DL models can also popularize and boost its application in the clinic[21].

ML models have also been relevant for the prediction of thin-cap fibroatheromas by co-registering OCT and IVUS frames[22]. As in this case, where OCT was leveraged by the data extracted from IVUS frames, DL models can be benefited by using ground truth data from complementary procedures. Using annotations taken from histopathological images, ML classifiers were tested for the prediction of plaque type in OCT images[23]. In turn, analysis of textures and perivascular image patterns from CT images enabled ML models to learn signatures present in perivascular adipose tissue to predict cardiac risk, providing comprehensive image-based analysis beyond conventional calcium score, coronary stenosis and high-risk plaque features[24].

The characterization of atherosclerotic plaque is intrinsically associated to the extraction of precise morphological and morphometric features from medical images. This procedure amounts to perform accurate image segmentation of vascular structures to identify those places within the vascular wall that are affected by the presence of atherosclerotic plaque, in addition to the identification of stenoses, and eventually the quantification of calcium score and other plaque features[25]. The problem grows in complexity when the goal is to track in time the progression/regression of a given plaque, because the interest shifts from absolute measurements regarding the plaque to differential measurements between two time points. Using AI for the assessment of medical images towards this end becomes extremely challenging, because of the very complexity of such a quantification procedure, and also because of the large inter-

individual and even intra-individual variability in these evaluations.

The application of AI to the analysis of coronary atherosclerotic plaque has been abundant along the last years. ML models nurtured by OCT, IVUS, and CCTA, have been developed to localize atherosclerotic plaque in coronary vessels, classify types of plaques, and analyze plaque vulnerability[26]. State-of-the-art ML models depend upon the model outcome. **Figure 1** Aiming at an automated radiomic analysis of medical images, the framework provided by DL has dominated the landscape. By exploiting convolutional neural networks, these DL aim at extracting features that help the automated classification of plaques, computation of coronary atherosclerotic calcium scores, and detection of non-obstructive disease, among others[27]. If the goal is to diagnose the existence of a certain condition, or to predict risk of adverse cardiovascular events, clustering techniques such as support vector machines, random forest algorithms, XGBoost, and other ensemble methods have been employed successfully.

REFERENCES

1. Asakura T, Karino T. Flow patterns and spatial distribution of atherosclerotic lesions in human coronary arteries. Circ Res. 1990 Apr;66(4):1045–66.

2. Pu J, Mintz GS, Biro S, Lee JB, Sum ST, Madden SP, et al. Insights Into Echo-Attenuated Plaques, Echolucent Plaques, and Plaques With Spotty Calcification. Journal of the American College of Cardiology. 2014 Jun;63(21):2220–33.

3. Jinnouchi H, Sato Y, Torii S, Sakamoto A, Cornelissen A, Bhoite RR, et al. Detection of cholesterol crystals by optical coherence tomography. EuroIntervention. 2020 Aug;16(5):395–403.

4. Ahmadi A, Stone GW, Leipsic J, Shaw LJ, Villines TC, Kern MJ, et al. Prognostic Determinants of Coronary Atherosclerosis in Stable Ischemic Heart Disease: Anatomy, Physiology, or Morphology? Circ Res. 2016 Jul 8;119(2):317–29.

5. Virmani R, Kolodgie FD, Burke AP, Farb A, Schwartz SM. Lessons from sudden coronary death: a comprehensive morphological classification scheme for atherosclerotic lesions. Arterioscler Thromb Vasc Biol. 2000 May;20(5):1262–75.

6. Yahagi K, Kolodgie FD, Otsuka F, Finn AV, Davis HR, Joner M, et al. Pathophysiology of native coronary, vein graft, and in-stent atherosclerosis. Nat Rev Cardiol. 2016 Feb;13(2):79–98.

7. Kolodgie FD, Gold HK, Burke AP, Fowler DR, Kruth HS, Weber DK, et al. Intraplaque Hemorrhage and Progression of Coronary Atheroma. N Engl J Med. 2003 Dec 11;349(24):2316–25.

8. Mann J, Davies MJ. Mechanisms of progression in native coronary artery disease: role of healed plaque disruption. Heart. 1999 Sep 1;82(3):265–8.

9. Burke AP, Kolodgie FD, Farb A, Weber DK, Malcom GT, Smialek J, et al. Healed plaque ruptures and sudden coronary death: evidence that subclinical rupture has a role in plaque progression. Circulation. 2001 Feb 20;103(7):934–40.

10. Vergallo R, Crea F. Atherosclerotic Plaque Healing. N Engl J Med. 2020 Aug 27;383(9):846–57.

11. Torii S, Jinnouchi H, Sakamoto A, Kutyna M, Cornelissen A, Kuntz S, et al. Drug-eluting coronary stents: insights from preclinical and pathology studies. Nat Rev Cardiol. 2020 Jan;17(1):37–51.

12. Garcia-Garcia HM, Muramatsu T, Nakatani S, Lee IS, Holm NR, Thuesen L, et al. Serial optical frequency domain imaging in STEMI patients: the follow-up report of TROFI study. European Heart Journal - Cardiovascular Imaging. 2014 Sep 1;15(9):987–95.

13. Glagov S, Weisenberg E, Zarins CK, Stankunavicius R, Kolettis GJ. Compensatory enlargement of human atherosclerotic coronary arteries. N Engl J Med. 1987 May 28;316(22):1371–5.

14. Maurovich-Horvat P, Ferencik M, Voros S, Merkely B, Hoffmann U. Comprehensive plaque assessment by coronary CT angiography. Nat Rev Cardiol. 2014 Jul;11(7):390–402.

15. Cury RC, Leipsic J, Abbara S, Achenbach S, Berman D, Bittencourt M, et al. CAD-RADS™ 2.0 - 2022 Coronary Artery Disease-Reporting and Data System. Journal of Cardiovascular Computed Tomography. 2022 Nov;16(6):536–57.

16. Kubo T, Imanishi T, Takarada S, Kuroi A, Ueno S, Yamano T, et al. Assessment of culprit lesion morphology in acute myocardial infarction: ability of optical coherence tomography compared with intravascular ultrasound and coronary angioscopy. J Am Coll Cardiol. 2007 Sep 4;50(10):933–9.

17. Byrne RA, Rossello X, Coughlan JJ, Barbato E, Berry C, Chieffo A, et al. 2023 ESC Guidelines for the management of acute coronary syndromes. European Heart Journal. 2023 Aug 25;ehad191.

18. Tuzcu EM, Kapadia SR, Tutar E, Ziada KM, Hobbs RE, McCarthy PM, et al. High prevalence of coronary atherosclerosis in asymptomatic teenagers and young adults: evidence from intravascular ultrasound. Circulation. 2001 Jun 5;103(22):2705–10.

19. Gary S. Mintz, Hector M. Garcia-Garcia, Stephen J. Nicholls, Neil J. Weissman, Nico Bruining, Tim Crowe, et al. Clinical expert consensus document on standards for acquisition, measurement and reporting of intravascular ultrasound regression/progression studies. EuroIntervention. 2011 Apr 20;6(9):1123–30.

20. Choi AD, Marques H, Kumar V, Griffin WF, Rahban H, Karlsberg RP, et al. CT Evaluation by Artificial Intelligence for Atherosclerosis, Stenosis and Vascular Morphology (CLARIFY): A Multi-center, international study. Journal of Cardiovascular Computed Tomography. 2021 Nov;15(6):470–6.

21. Kolossváry M, Karády J, Szilveszter B, Kitslaar P, Hoffmann U, Merkely B, et al. Radiomic Features Are Superior to Conventional Quantitative Computed Tomographic Metrics to Identify Coronary Plaques With Napkin-Ring Sign. Circ: Cardiovascular Imaging. 2017 Dec;10(12):e006843.

22. Bae Y, Kang SJ, Kim G, Lee JG, Min HS, Cho H, et al. Prediction of coronary thin-cap fibroatheroma by intravascular ultrasound-based machine learning. Atherosclerosis. 2019 Sep;288:168–74.

23. Bajaj R, Eggermont J, Grainger SJ, Räber L, Parasa R, Khan AHA, et al. Machine learning for atherosclerotic tissue component classification in combined near-infrared spectroscopy intravascular ultrasound imaging: Validation against histology. Atherosclerosis. 2022 Mar;345:15–25.

24. Oikonomou EK, Williams MC, Kotanidis CP, Desai MY, Marwan M, Antonopoulos AS, et al. A novel machine learning-derived radiotranscriptomic signature of perivascular fat improves cardiac risk prediction using coronary CT angiography. European Heart Journal. 2019 Nov 14;40(43):3529–43.

25. Covas P, De Guzman E, Barrows I, Bradley AJ, Choi BG, Krepp JM, et al. Artificial Intelligence Advancements in the Cardiovascular Imaging of Coronary Atherosclerosis. Front Cardiovasc Med. 2022 Mar 21;9:839400.

26. Zhang J, Han R, Shao G, Lv B, Sun K. Artificial Intelligence in Cardiovascular Atherosclerosis Imaging. JPM. 2022 Mar 8;12(3):420.

27. Kampaktsis PN, Emfietzoglou M, Al Shehhi A, Fasoula NA, Bakogiannis C, Mouselimis D, et al. Artificial intelligence in atherosclerotic disease: Applications and trends. Front Cardiovasc Med. 2023 Jan 19;9:949454.

Table 1. Tissue types: preferred descriptive names.

	IVUS*	OCT	CCTA**
Lipid	Hypoechogenic With/without Attenuation	Hyporeflective With Diffuse Contours	Low density (low HU^)
Calcium	Hyperechogenic With Acoustic Shadow	Hyporeflective With Sharp Contours	High density (high HU)
Fibrous	Normoechogenic	Hyperreflective	Intermediate density

* Echogenicity is assed by comparing the plaque appearance with the adventitia

** CCTA is computed coronary tomography angiography.
^ HU is Hounsfield Units

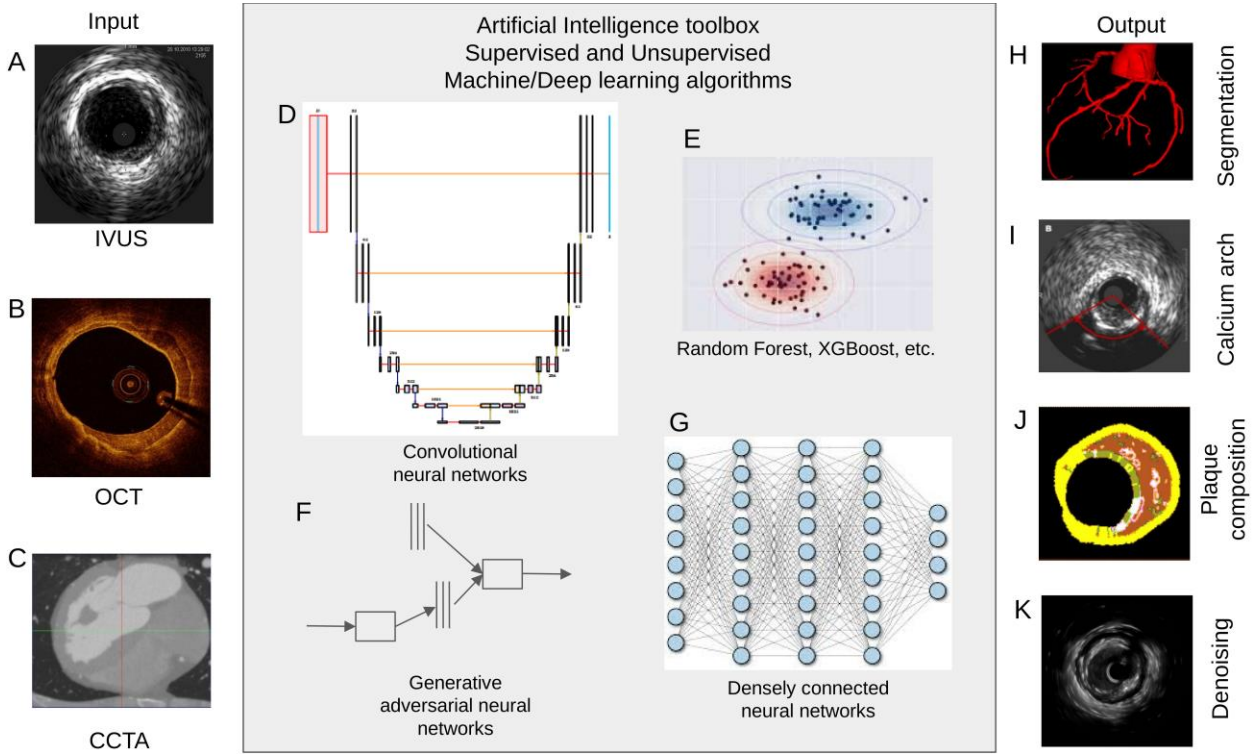

Figure 1. **Machine learning machinery applied to imaging of atherosclerosis.**

Input data to algorithms are in the form of sets of IVUS pullbacks, (panel A) OCT pullbacks (panel B), as well as CCTA volumes (panel C). ML algorithms such as random forest (panel E) can be employed to diagnose existence or not of a certain condition, or type of plaque, while DL models, such as convolutional neural networks (panel D), fully connected neural networks (panel G), and adversarial neural networks (panel F) are used to perform image segmentation tasks (panel H), analyze plaque composition (panel J), quantify calcium score and arch extension (panel I), and even to remove artifacts and denoise images (panel K).